
Article:
Wu, X., Wang, M. orcid.org/0000-0001-9752-270X, Shen, J. et al. (3 more authors) (2019) Reinforced coordinated control of coal-fired power plant retrofitted with solvent based CO2 capture using model predictive controls. Applied Energy, 238. pp. 495-515. ISSN 0306-2619

https://doi.org/10.1016/j.apenergy.2019.01.082

Reinforced Coordinated Control of Coal-fired Power Plant Retrofitted with Solvent Based CO_2 Capture using Model Predictive Controls

Xiao Wu[a,*], Meihong Wang[b,*], Jiong Shen[a], Yiguo Li[a],
Adekola Lawal[c], Kwang Y. Lee[d]

[a]Key laboratory of Energy Thermal Conversion and Control of Ministry of Education , Southeast Univerisity, Nanjing 210096, China
[b]Department of Chemical and Biological Engineering, Univerisity of Sheffield, Sheffield S1 3JD, UK
[c]Process Systems Enterprise Ltd, 26-28 Hammersmith Grove, London W6 7HA, UK
[d]Department of Electrical and Computer Engineering, Baylor University, One Bear Place #97356, Waco, TX 76798-7356, USA

Abstract

Solvent-based post-combustion CO_2 capture (PCC) provides a promising technology for the CO_2 removal of coal-fired power plant (CFPP). However, there are strong interactions between the CFPP and the PCC system, which makes it challenging to attain a good control for the integrated plant. The PCC system requires extraction of large amounts of steam from the intermediate/low pressure steam turbine to provide heat for solvent regeneration, which will reduce power generation. Wide-range load variation of power plant will cause strong fluctuation of the flue gas flow and brings in a significant impact on the PCC system. To overcome these issues, this paper presents a reinforced coordinated control scheme for the integrated CFPP-PCC system based on the investigation of the overall plant dynamic behavior. Two model predictive controllers are developed for the CFPP and PCC plants respectively, in which the steam flow rate to re-boiler and the flue-gas flow rate are considered as feed-forward signals to link the two systems together. Three operating modes are considered for designing the coordinated control system, which are: 1) normal operating mode; 2) rapid power load change mode; and 3) strict carbon capture mode. The proposed coordinated controller can enhance the overall performance of the CFPP-PCC plant and achieve a flexible trade-off between power generation and CO_2 reduction. Simulation results on a small-scale subcritical CFPP-PCC plant developed on gCCS demonstrates the effectiveness of the proposed controller.

Keywords: Coal-fired power plant; Solvent-based post-combustion carbon capture; Coordinated control; Model predictve control.

1. Introduction

1.1 Background and motivation

Rising sea level and frequent flooding are fast becoming big threats to the economy and society around the world [1]. At the United Nations Framework Convention on Climate Change (UNFCCC) held in Paris in Dec. 2015, a common goal was agreed by the all the 196 parties to keep global warming to less than 2°C in 2050 compared to pre-industrial levels [2]. In line with this ambitious target, countries seek to develop technologies that will reduce CO_2 emissions from coal-fired power plants (CFPP). In China, there are over 900 gigawatts (GWe) of installed coal-fired power plants representing almost 50% of the global total and still has nearly 200 GWe under construction [3]. Two-thirds of these plants were built after 2005 and most of them could run for another three to four decades [3]. For this reason, while extensively promoting the renewable energy and making effort to improve the efficiency of CFPPs, CO_2 capture from CFPPs has been recognized as the most effective and direct way to achieve a large-scale CO_2 emission reduction in the future 30 years [3].

Compared with many other CO_2 capture methods, the solvent-based post-combustion CO_2 capture (PCC) can directly remove the low concentration CO_2 from flue gas, which is mature in technology, relatively low in cost and easily retrofitted for existing power plants. Therefore, it has been viewed as the most suited technology for power plant CO_2 capture and may be deployed extensively in future [4].

For the integrated CFPP-PCC system, its operating characteristics are quite different from those of individual CFPP:

(1) Operation of the carbon capture plant requires extraction of large amounts of steam from the intermediate pressure (IP)

* Corresponding author.
E-mail address: wux@seu.edu.cn (X. Wu); Meihong.Wang@sheffield.ac.uk (M. Wang)

/low pressure (LP) turbine to provide heat for solvent regeneration. Although integration of PCC unit can achieve better environmental benefits, it will increase energy consumption and reduce power generation efficiency [4];

(2) The extensive use of intermittent renewable sources such as solar and wind in the power grid forces the CFPP to participate in the grid power regulation frequently and quickly in a wide range of load. The integration of PCC unit will enhance the CFPP's load tracking performance because changing the extracted steam flow rate can quickly achieve a tradeoff between power generation and CO_2 reduction [5];

(3) During the wide range of CFPP load change, the fluctuation of flue gas flow rate will severely affect the operation of PCC process [6]; and

(4) The two-system integration will increase complexity of the entire plant. As a result, the couplings among multi-variables and large inertia behavior of the system becomes stronger and thus is more difficult to control [7].

In summary, the need for flexible operation increases the control requirements of the CFPP-PCC integrated plant on one hand; and on the other hand, the strong interactions between the CFPP and PCC systems increase the difficulty in control. A simple combination of CFPP control scheme with an independent PCC control cannot effectively handle the couplings among multi-variables within the integrated system to achieve a satisfactory control performance. Therefore, an in-depth study of the dynamic characteristics of the overall CFPP-PCC unit and developing an appropriate coordinated control technique is of great significance for the optimal and flexible operation of the integrated plant.

1.2 Literature review

Research on dynamic operation and control of the integrated CFPP-PCC system is still in its infant stage. From the optimization point of view, almost all of the current research adopts a steady-state optimization scheme at a given operating condition. Aroonwilas and Veawab [8] carried out static simulation on a 500MWe supercritical CFPP retrofitted with PCC, the influence of some key parameters on the power plant efficiency, coal combustion rate and amounts of CO_2 captured was studied. These parameters include: CO_2 capture level, coal quality, flue gas delivery scheme, solvent selection and re-boiler steam pressure.

Similarly, Cifre et al. [9] developed steady-state models for both 600MWe and 1000MWe power stations integrated with CO_2 capture and compression devices, and they studied the influence of PCC process parameters such as absorber/stripper sizes, solvent flow rate and operating temperature/pressure on the power plant performance.

Sanpasertparnich et al. [10] undertook steady-state simulation of an 800MWe supercritical CFPP retrofitted with PCC. They investigated the performance of the entire plant under different coal grades, re-boiler steam parameters and power plant loading conditions. The results show that at lower loading conditions, the energy consumptions of the PCC plant are relatively higher.

To investigate the techno-economic impact of integrated CFPP-PCC unit on the net power plant efficiency, Oh, Yun and Kim [11] simulated a 550MWe supercritical CFPP together with CO_2 capture and compression process in Aspen Plus. Steady-state simulation based parameter optimization and process modification were carried out to minimize the heat required for CO_2 removal. Moreover, advanced integration options for minimizing the net efficiency penalty were proposed by exploiting the choice of steam quality for solvent regeneration.

In Lucquiaud, Chalmers and Gibbins [12], three steam turbine retrofit options for steam extraction of PCC unit were studied, which are Clutched LP turbine, Throttled LP Turbine and Floating IP/LP crossover pressure. The last two options are shown to have lower cost and better flexibility. Fernandez et al. [5] pointed out that the power generation penalty of CO_2 capture and compression increases at partial load, compared with that at the full load. However, it is possible to improve the efficiency of the entire PCC-retrofitted power plant under partial-load condition by jointly designing the whole system using an advanced operation mode.

Rio, Gibbins and Lucquiaud [13] presented a new integration approach for the PCC-retrofitted power plant. The flue gas of gas turbine is fed into the boiler via the wind-box for sequential combustion to allow CO_2 capture in a single dedicated PCC plant. The resulting lower flue gas flow rate and higher CO_2 concentration decreases the energy penalty of CO_2 capture for the integrated plant. Wang et al. [14] proposed to upgrade the low-temperature steam of turbine to match the requirement of PCC re-boiler using a double absorption heat transformer; thus reduce the thermal energy loss, which was caused by unmatched temperature difference between the extracted steam and the solvent.

Pan et al. [15] developed optimal methodologies in retrofitting natural gas combined cycle power plants with CO2 capture. Suitable steam from the heat recovery steam generator is extracted to provide heat for the capture process. In addition, the technique of exhaust gas recirculation is employed, which can increase the power plant efficiency and reduce the heat demands of the PCC plant. Adams and Mac Dowell [16] presented a 420MWe triple-pressure combined cycle gas turbine power plant model and integrated it with a solvent based PCC process model. The effect of exhaust gas recirculation on the process performance was studied and moreover, the economic performance of the whole plant under full and part operating conditions was evaluated.

During the daily operation, the CFPP has to change the generation frequently in a wide range to meet the grid demand [17]. Due to the high energy requirement of the CO_2 capture, the PCC unit also has to change the capture level quickly to achieve a tradeoff between the power generation and the CO_2 reduction. Flexible operation has drawn much attention and has been recognized as a key step towards the wide-range application for the CFPP-PCC technology. However, the aforementioned steady-state studies have neither considered, nor optimized, the dynamic performance of the CFPP-PCC plant during the load varying operation.

From the systems point of view, most of the research on dynamic systems have focused on the PCC system alone, but its integration with the CFPP has not been taken into account. Simulation studies based on the first-principle models of the PCC process were carried out in [18] and [19], where the dynamic relationships among the core variables were analyzed. Instead of complex analytical model, data-driven models were developed through identification to investigate the characteristics of the PCC process in [20] and [21]. Dynamic performance of PCC unit were studied in [22] and [23] via open-loop step response tests on pilot plants, where the slow dynamic feature of the PCC process was clearly demonstrated.

Wu et al. [24] investigated the dynamic behavior of the PCC unit caused by the variation of key operational variables, such as CO_2 capture level, flue gas flow rate and re-boiler temperature. Simulation results showed that the variation of the PCC dynamics is quite apparent around the optimal re-boiler temperature point.

Based on the understanding of the PCC process dynamics, decentralized proportional-integral (PI) controllers were developed in [25]-[27]. To attain a quick regulation on the CO_2 capture level, a typical control structure was selected in these studies, which used the lean solvent flow rate and the steam flow rate to re-boiler to control, respectively, the capture level and the re-boiler temperature.

To enhance the flexible control performance of the PCC process, model predictive control (MPC) was developed in [6], [24], [29]-[31] instead of conventional PI controls. By using a PCC dynamic model to predict the future output of the plant, the control input sequence that can produce the most desired output response is computed at each sampling time. Owing to the outstanding ability of the MPC in handling slow dynamics, strong couplings and stringent constraints, better capture level tracking and re-boiler temperature regulation were reported in comparison with the performance of PI controls.

Although in some studies, the impact of the flue gas changes on the PCC operation was considered in controller design or tests, the dynamic influence of the PCC operation on the power plant was not considered. The variation of steam flow rate to re-boiler will greatly change the power generation of the CFPP. Therefore, controlling the PCC unit alone cannot comprehensively handle the interactions between the two systems and maximize the effectiveness of the entire CFPP-PCC unit in terms of power generation and emission reduction.

Lawal et al. [7] developed a dynamic model for a 500MWe subcritical CFPP with the PCC plant. Dynamic simulations were carried, which revealed the different responses of the two plants and the interactions between CO_2 capture and power generation. Independent controls, for each of the CFPP and PCC systems, were developed in this work.

Olaleye et al. [32] linked an industrial-size PCC model with a 600MWe supercritical CFPP model. The re-boiler steam drawn-off from the IP/LP crossover of the steam turbine was reduced or stopped temporarily to quickly generate more power in the case of urgent changes in the unit load demand for grid power regulation.

One limitation of these two studies is that, the dynamic models of coal mill system and the coal-flue gas channel were not considered. As a result, the dynamic process of the flue gas generation, which is strongly coupled with the downstream PCC plant, cannot be described. Moreover, simplified decentralized controllers were used in these works, which had negative effect on the operation of the integrated system. Therefore, advanced control design techniques should be developed to improve the performance of the complex CFPP-PCC integrated system.

1.3 Novel contributions

This paper proposes a reinforced coordinated control system for flexible operation of the CFPP-PCC plant as a whole. The main contributions and novelties of the paper are:

1) the dynamic behavior of the integrated CFPP-PCC system is investigated for the purpose of control system design;

2) a reinforced coordinated control scheme is proposed, which can greatly enhance the overall performance of the CFPP-PCC plant; and

3) three operating modes are considered for designing the coordinated control, so that the entire CFPP-PCC system works effectively for both power generation and CO_2 reduction.

The proposed coordinated control system structure is illustrated in Fig. 1, which is composed of two sub-MPCs: power plant MPC and capture plant MPC.

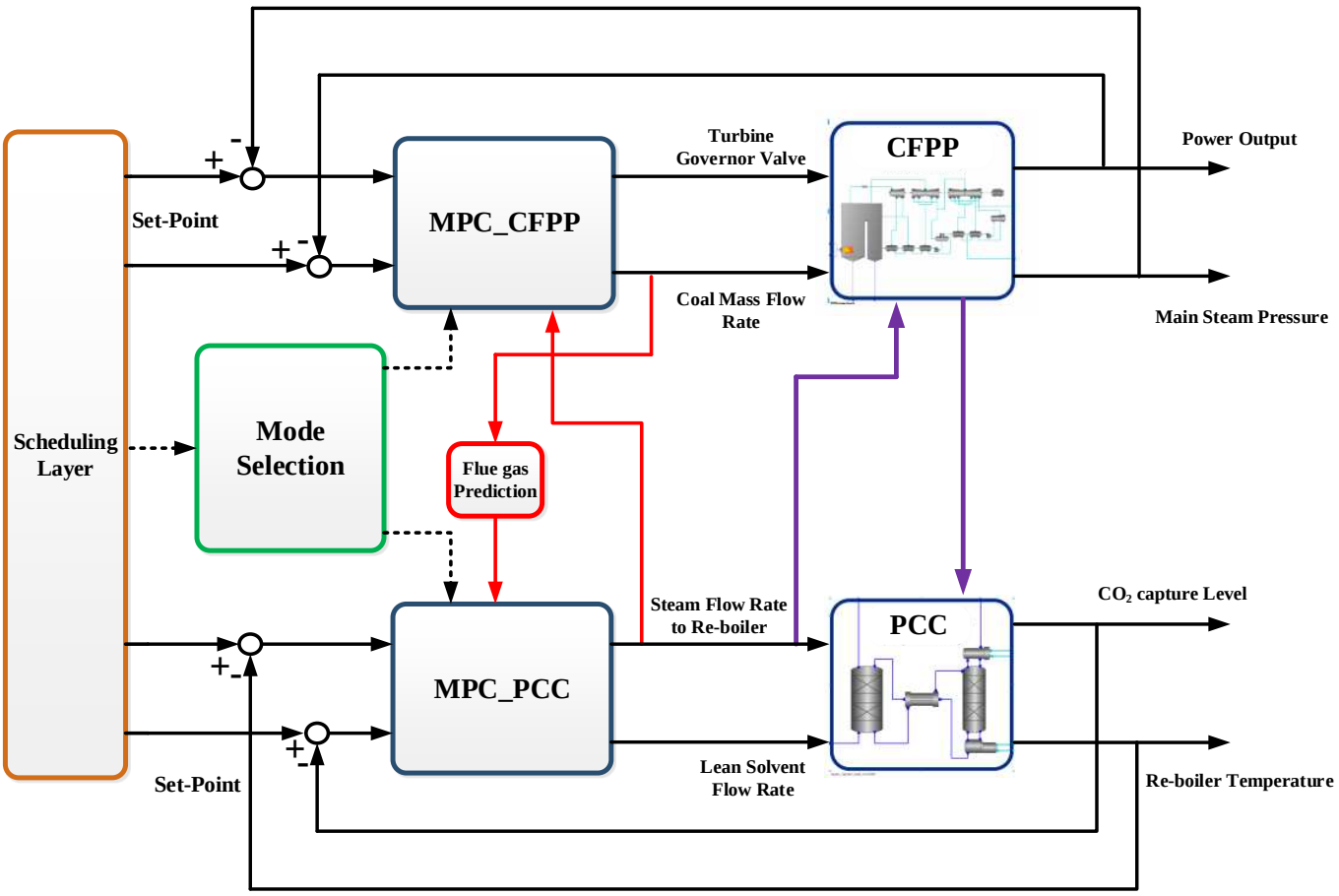

Fig. 1. Schematic diagram of the proposed coordinated control system structure for the integrated CFPP-PCC system.

The MPC for CFPP runs with a small sampling period since the response of CFPP is quicker than that of the PCC unit. In addition to the conventional CFPP boiler-turbine controller, which uses coal mass flow rate and turbine governor valve position to control the power output and main steam pressure, this MPC utilizes the current and future predicted steam flow rates to re-boiler as feedforward signals, so that the impact of PCC operation on CFPP can be known in advance and compensated.

The MPC for PCC operates with a large sampling time since PCC has relatively slow dynamics. Based on the conventional PCC controller design, which uses lean solvent flow rate and steam flow rate to re-boiler to control the CO_2 capture level and re-boiler temperature, this MPC utilizes the flue gas flow rate of CFPP as a feedforward signal so that the PCC system can quickly adapt to the load variation of CFPP. Unlike an individual PCC control system design, which only uses the flue gas flow rate measured at current time as feedforward signal, the future flue gas flow rate is also predicted via the past coal mass flow rate and used in the MPC_PCC development. The designed MPC_PCC can thus achieve a better control performance.

The use of feedforward signals links the CFPP and PCC systems together and makes the present and pending actions of the two systems known to each other in advance. Therefore, the interactions between the two systems can now be fully utilized to improve the flexible operating performance of the overall plant. Three operating modes focusing on different control targets are then considered for designing the coordinated controller, which are: 1) normal operating mode; 2) accelerated load change mode; and 3) strict carbon capture mode.

1.4 Outline of the paper

Section 1 introduced the background, motivation and contributions of this work. Section 2 briefly describes the integrated CFPP-PCC process, and the dynamic performance of the overall system is investigated in Section 3. Section 4 presents the reinforced coordinated control scheme design for the integrated CFPP-PCC plant, and simulation results are shown in Section 5. Conclusions are drawn in Section 6.

2. System Description

The PCC dynamic model in this paper is developed based on the pilot plant presented in [25], [33] and [34] using gCCS toolkit [35], which is a commercial software specifically used for CO_2 capture, transportation and storage simulation. The PCC plant uses 30wt% monoethanolamine (MEA) solvent as the chemical sorbent and is capable of treating 0.13kg/s flue gas with CO_2 concentration of 25.2wt% under nominal condition. The specification and parameters of the major devices are set according to the model developed in [25], which has been validated through pilot scale experimental data to provide high-fidelity description of this capture process.

In order to match the PCC unit, a simplified model of a small scale subcritical CFPP is developed according to the basic equations given in [7] and [32]. To better reflect the interactions between the CFPP and PCC systems, the coal mill system, which reflects the main dynamics of the coal/air-flue gas channel, is taken into account as modification based on the modeling method given in [36]. The dynamic relationships between coal and the generated flue gas, as well as its influence on the PCC system, can thus be reflected clearly through this model. Although the CFPP model is simplified and small in scale, it can describe the typical characteristics of the boiler-turbine unit.

To link the CFPP and PCC systems together, the following assumptions are made: 1) the flue gas is assumed to be desulfurized, denitrified, dust removed and cooled down to 40 ℃ before being fed into the absorber; 2) the steam to the re-boiler is drawn at the IP/LP crossover of the turbine and is assumed to be well maintained at 3bar, 410K by additional controls; and 3) the condensate water of re-boiler steam returns to the feed-water system, and the feed-water temperature is assumed to be constant through regulation of the reheating system. The process topology of the CFPP-PCC integrated system is presented in Fig. 2. Some key operating parameters under nominal operating condition are given in Table 1.

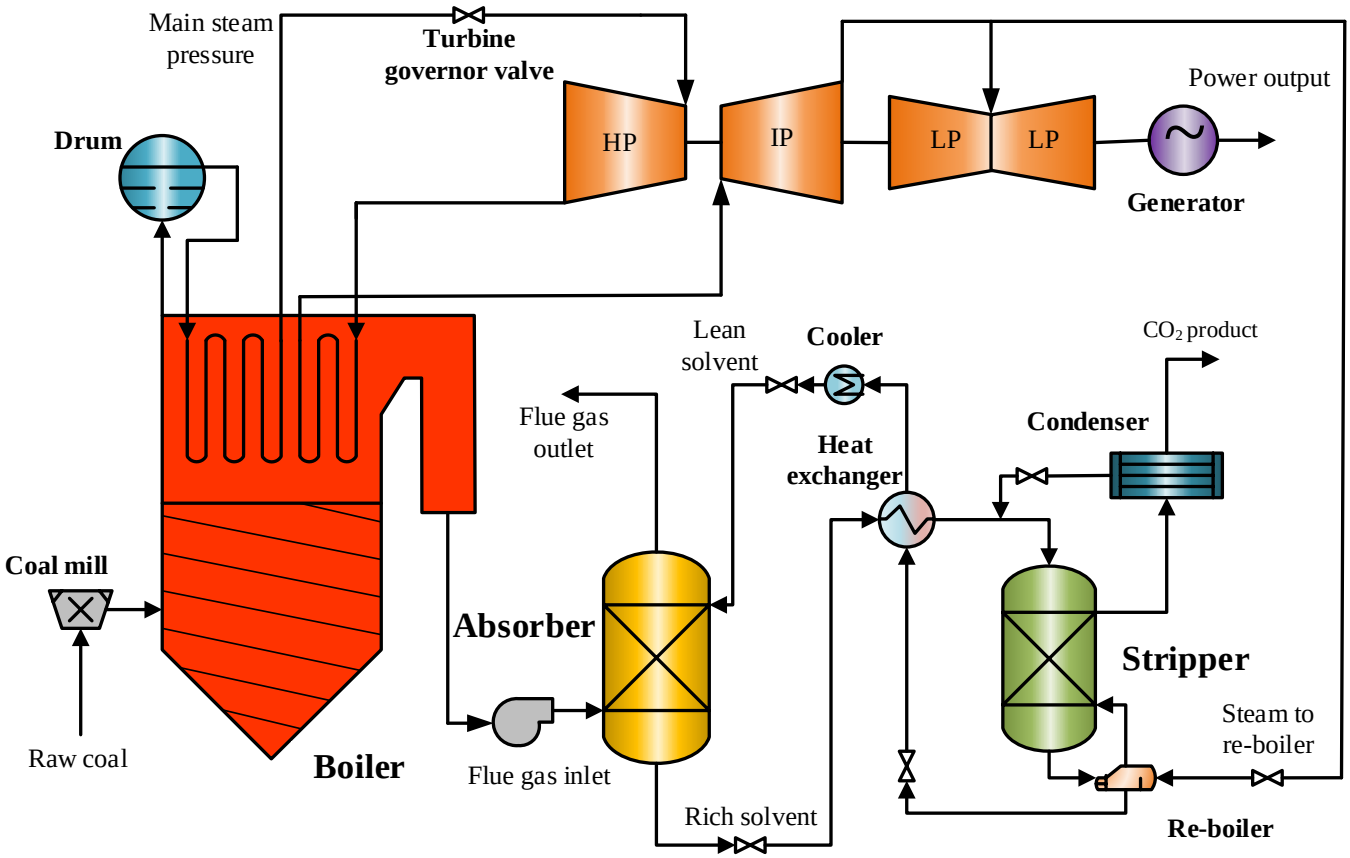

Fig. 2. Process topology of CFPP-PCC integrated system.

Table 1. Nominal Operating Condition of Key Variables for the integrated CFPP-PCC Model Developed in gCCS

Variable	Unit	Value
Power output	[MWe]	0.175
Turbine governor valve position	[%]	81.09
Coal mass flow rate	[kg/s]	0.0234
Drum Pressure	[MPa]	15.41
Main steam pressure	[MPa]	14.76
Flue gas flow rate	[kg/s]	0.1261
Flue gas CO_2 concentration	[wt%]	25.2
Steam flow rate to re-boiler	[kg/s]	0.0462
Re-boiler steam pressure	[MPa]	0.3
Re-boiler steam temperature	[K]	410
Flue gas absorber inlet temperature	[K]	313.15
Solvent flow rate	[kg/s]	0.5464
MEA concentration	[wt%]	30
Re-boiler pressure	[bar]	1.79
Re-boiler temperature	[K]	386
Condenser Pressure	[bar]	1.69
Condenser temperature	[K]	313.15
CO_2 capture level*	[%]	90

$$* \text{CO}_2 \text{ Capture Level} = \frac{\text{CO}_2 \text{ in the flue gas} - \text{CO}_2 \text{ in the clean gas}}{\text{CO}_2 \text{ in the flue gas}}$$

The CFPP control schemes have undergone several decades of development and evolution. Two primary objectives of the CFPP are: i) following the unit power load demand at all times, and ii) balancing the boiler's steam flow supply with the turbine's energy requirement to guarantee a safe and economical operation of the plant. Therefore, the power output and the main steam pressure are viewed as the most important controlled variables (CVs). The coal mass flow rate and the turbine governor valve are selected as the manipulated variables (MVs). These four variables are in the upper most layer of CFPP control [37].

Regarding the PCC system control, the CO_2 capture level and the re-boiler temperature are considered as the most central CVs [24]-[31]. The capture level indicates the degree of CO_2 removal from the flue gas. The re-boiler temperature reflects the CO_2 loading of regenerated lean solvent, which determines the CO_2 absorption ability. Moreover, a solvent degradation will occur under an excessively high re-boiler temperature. The lean solvent flow rate and the re-boiler steam flow rate drawn off from the turbine are selected as the MVs.

Regarding the interaction of the integrated CFPP-PCC system, the steam flow rate to the PCC re-boiler will also influence the power output of the CFPP, and the CFPP flue gas flow rate, which is decided by the coal mass flow rate, has a significant impact on the operation of PCC plant. Therefore, special attention needs to be paid on these two variables.

Based on the above analysis, the dynamics and interactions among key variables within the CFPP-PCC are first investigated and a reinforced coordinated control structure is then proposed to enhance the operating performance of the overall CFPP-PCC system.

3. Dynamic Behavior Analysis for the Integrated CFPP-PCC System

To develop an effective coordinated control strategy for the CFPP-PCC system, the dynamic behavior of the two units and the interactions among them are investigated through open-loop step response tests. At the nominal operating point given in Table 1, step signals are applied to the turbine governor valve, flue gas flow rate, coal mass flow rate, lean solvent flow rate and steam flow rate to re-boiler independently under open-loop condition, and their impact on the major CVs, power output, main steam pressure, flue gas flow rate, CO_2 capture level and re-boiler temperature, are shown in Figs. 3-7.

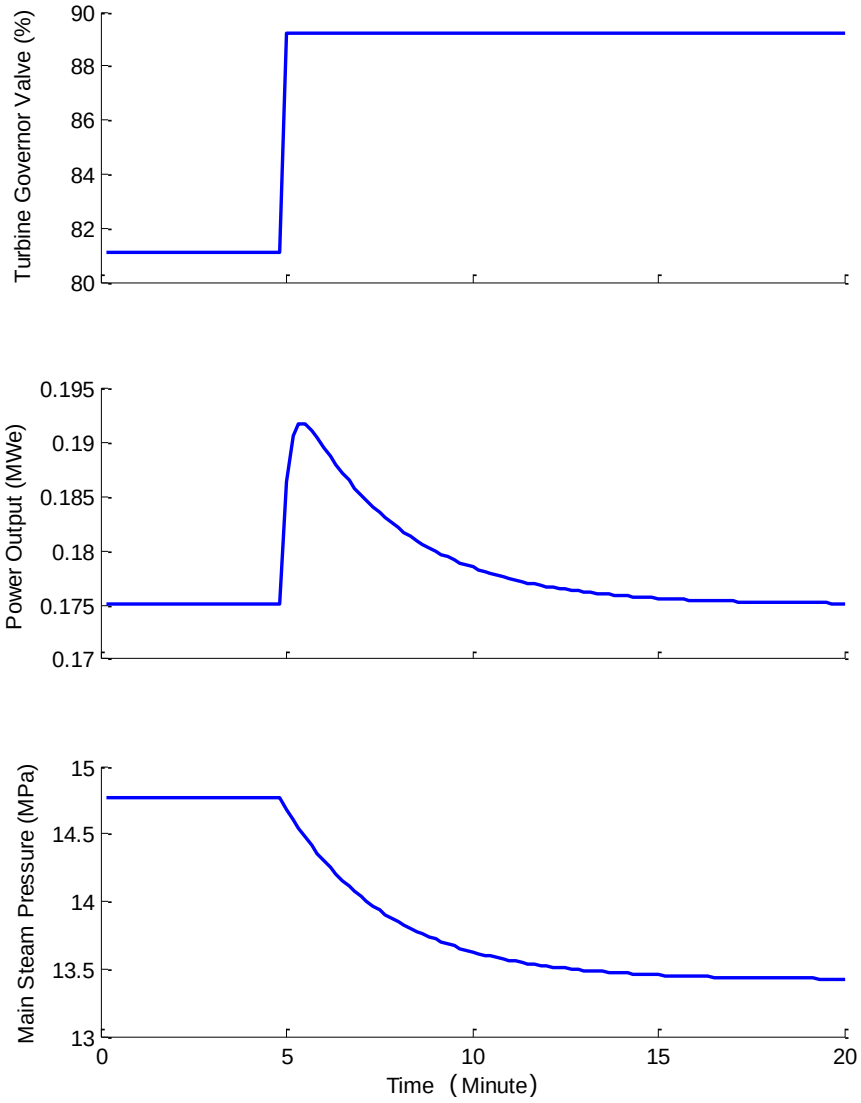

Fig. 3. Responses of the CFPP unit corresponding to +10% turbine governor valve step input.

The influence of turbine governor valve on the CFPP unit is illustrated in Fig. 3. At t=5 min, the turbine governor valve has increased by 10% in step. The increase of the turbine governor valve leads to the rapid increase in the main steam flow rate, thus the power output increases rapidly in about 30s. However, since there is no change in coal mass flow rate and the energy supply, this increase in power output is only temporary, which consumes the heat stored in the boiler. As the stored heat is gradually released, the main steam pressure is gradually reduced, and the power output gradually returns to its original level. The transient process lasts for around 10 min to enter the new steady state. The turbine governor valve has little impact on the operation of the PCC system.

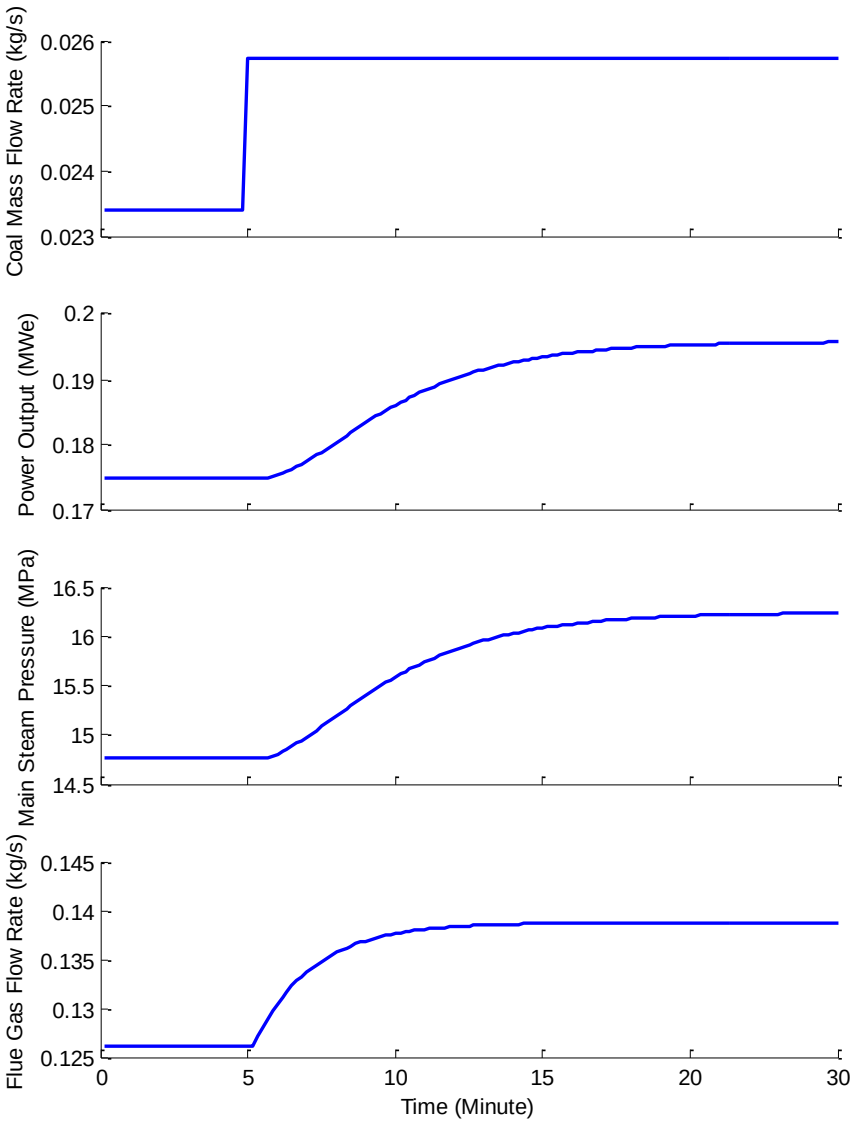

Fig. 4. Responses of the CFPP unit corresponding to +10% coal mass flow rate step input.

The influence of coal mass flow rate on the CFPP unit is illustrated in Fig. 4. The increase of coal mass flow rate will increase the steam generation of the boiler and increase the drum pressure and main steam pressure; the main steam flow rate will thus increase, resulting in power output increase. Due to the complex process of coal pulverization, combustion, flue gas flow and heat transfer, the impact of coal mass flow rate is slow compared to that of turbine valve. It takes about 15 min for the CFPP to enter the new steady state.

As shown in Fig. 4, the variation of coal mass flow rate will change the flue gas flow rate from the CFPP. Similar to the responses of power output and main steam pressure, the increase of flue gas flow rate is also slow because of the slow dynamics of the coal mill system. The whole transition process takes more than 10 min to finish. The flue gas flow rate has strong impact on the operation of PCC unit, which is illustrated in Fig. 5. Because the lean solvent and steam flow rates of PCC unit are at their original values, only a part of increased CO_2 in the flue gas can be captured. Thus, according to the definition of CO_2 capture level, the capture level will drop to a lower value quickly. Then as the rich solvent CO_2 loading is increased, the re-boiler temperature will slightly decrease and further decrease the CO_2 capture level, which is quite trivial.

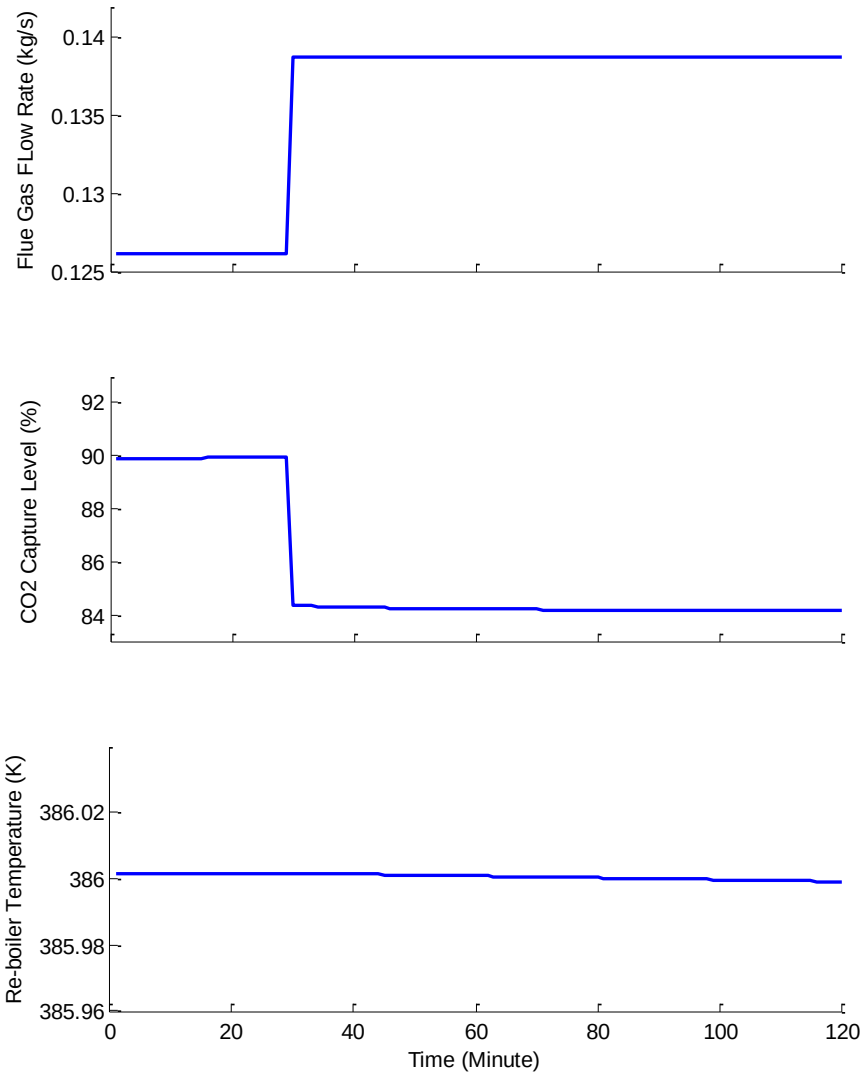

Fig. 5. Responses of the PCC unit corresponding to +10% flue gas flow rate step input.

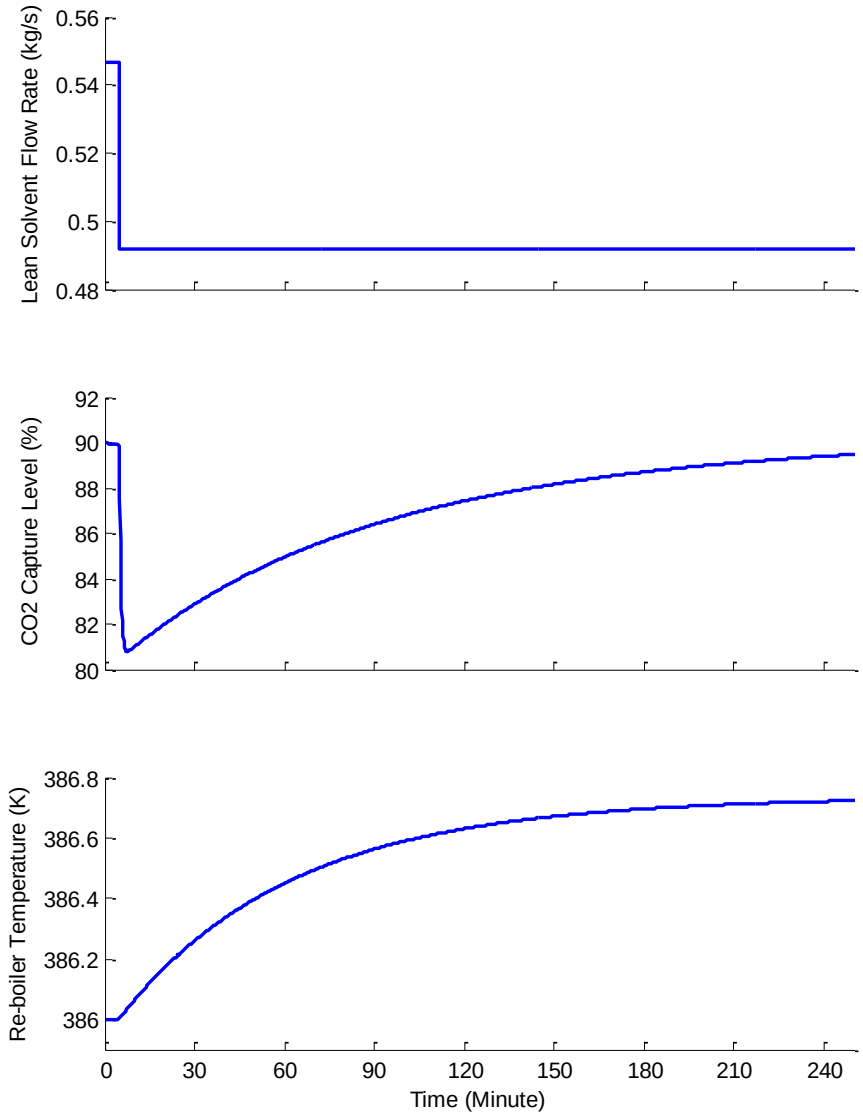

Fig. 6. Responses of the PCC unit corresponding to -10% lean solvent flow rate step input.

Fig. 6 describes the effect of lean solvent flow rate on the PCC system. As shown in Fig. 6, when less lean solvent is delivered into the absorber, less CO_2 in the flue gas can be absorbed temporarily and the CO_2 capture level decreases within 2-3 minutes. However, because the heat supplied to the re-boiler is not decreased, the CO_2 loading of lean-solvent is reduced, which enhances the CO_2 absorption ability of lean solvent. As a result, the capture level returns to the previous value gradually. The dynamics of the PCC system is very slow that more than 3 hours is required for the system to enter the new steady state.

On the other hand, as illustrated in Fig. 7, the re-boiler steam flow rate has effect on both the PCC and CFPP systems. For the PCC system, the decrease of steam flow rate to the re-boiler will decrease the re-boiler temperature first, which will then increase the CO_2 loading of lean solvent and finally decrease the CO_2 capture level. The response time of re-boiler temperature is shorter than that of capture level, but overall still very slow. For the CFPP system, the reduced steam to re-boiler will continue to work in the low pressure turbine, thus the power output can be rapidly increased in about 30s.

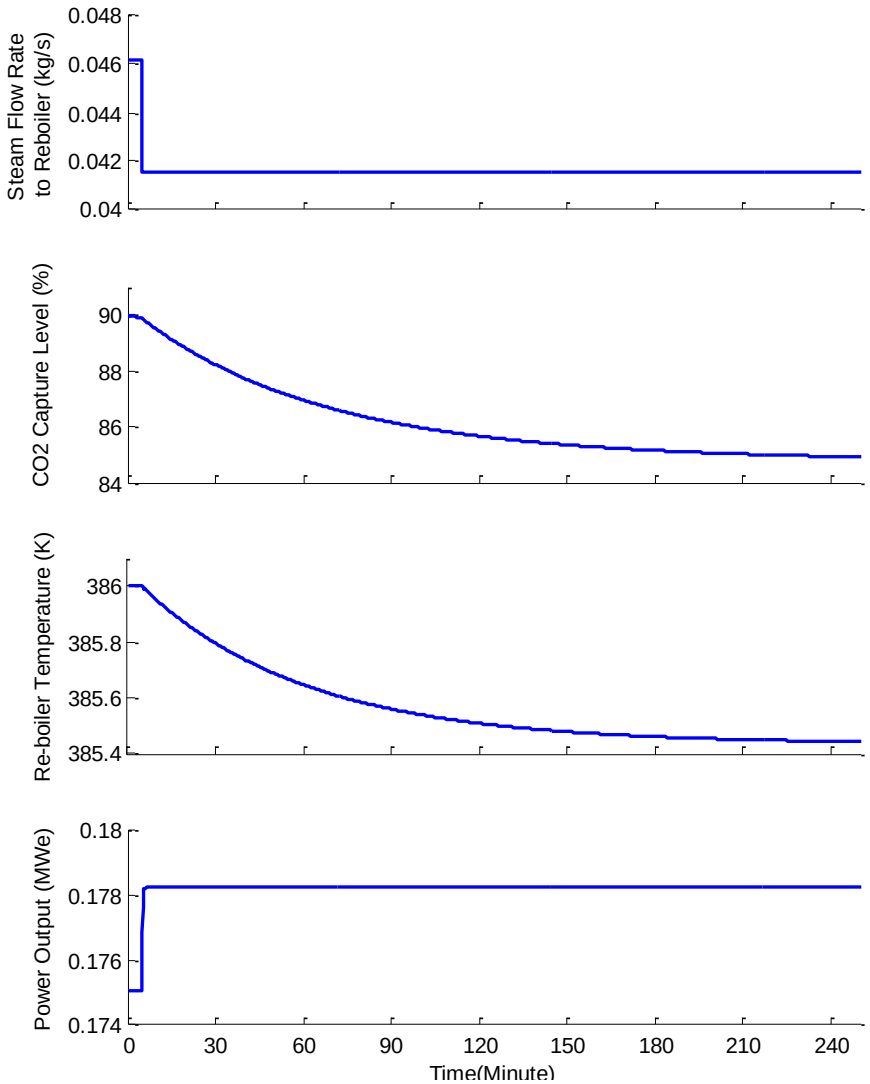

Fig. 7. Responses of the PCC and CFPP units corresponding to -10% steam flow rate to re-boiler step input.

The step response tests show that:

1) Both the CFPP and PCC systems exhibit typical inertial characteristics, and there are strong couplings among multi-variables within the respective systems;

2) The dynamic response time for the CFPP system is within 15 minutes, while the response time for the PCC system is more than 3 hours. The PCC system is much slower than the CFPP system;

3) There are strong interactions between the PCC and CFPP systems: The coal mass flow rate will change the flue gas flow rate and then influence the CO_2 capture level of the PCC process; The steam flow rate to re-boiler will change the power output of the CFPP rapidly.

Therefore, control of the CFPP-PCC system is of great challenge, and it is very important to establish an appropriate control system to utilize the interactions between the CFPP and PCC systems and to maximize the effectiveness of the integrated system in terms of power supply and CO_2 removal.

4. Reinforced Coordinated Control of the Integrated CFPP-PCC unit

4.1 Reinforced coordinated control system design for the CFPP-PCC unit

The investigation on dynamic behavior has provided a useful guidance for the CFPP-PCC system controller design. To deal with the large inertia and strong coupling characteristics of both systems, two MPCs are designed, one for each system, and set as the basis for the coordinated control system.

Another reason for choosing the MPC is that there are strict magnitude and rate constraints on the MVs of the CFPP-PCC system owning to the physical limitations of the valves. When these constraints are involved in the control implementation, performance degradation will occur for most of controllers. However, the MPC considers the influence of constraints in the controller design stage and provides the optimal control action in the presence of constraints.

Because the response speeds of the CFPP and PCC systems are quite different, different sampling times are set for each MPC. For the MPC_CFPP, as the turbine governor valve provides a very rapid response on the power output (shown in Fig. 3), we set the sampling time Ts_CFPP=10s; and for the MPC_PCC, although the whole transient process takes more than 3 hours to finish, the response of the capture level corresponding to the lean solvent flow rate change is very quick (shown in Fig. 6), thus we set the sampling time as Ts_CFPP=30s. Selecting excessively larger sampling times will make it difficult to capture these key dynamic features of CFPP and PCC systems, while selecting excessively smaller sampling times will catch too much system noise and increase the computational burden for the controller.

To make a better use of the interactions between the CFPP and PCC systems and combine them together, the flue gas flowrate and steam flow rate to re-boiler are utilized as additional feedforward signals in the PCC and CFPP controller designs, respectively. Different from the conventional design approaches, which only send the measured flue gas flow rate signals at current sampling time to the PCC controllers [24, 30], a method for deep reinforcement integration and coordination of the two systems is proposed in this paper. The method makes full use of the prediction feature of MPC, that takes the current and future estimation of flue gas and re-boiler steam flow rates as respective feedforward signals in MPC_PCC and MPC_CFPP developments. The future coal mass flow rate is predicted by the MPC_CFPP, from which the future flue gas flow rate is estimated. The future steam flow rate to re-boiler can be predicted by the MPC_PCC at each sapling time. The working principle of the entire coordinated control system is shown in Fig. 1.

State-space model based multi-variable design approach is used in both MPC designs, which consist of three parts:

A. Model prediction

State-space model that is convenient for multi-variable controller design is selected as the prediction model:

$$\begin{cases} x_{k+1} = Ax_k + Bu_k + Ef_k \\ y_k = Cx_k + Du_k + Ff_k \end{cases} \tag{1}$$

where x_k, u_k, y_k, f_k are the state, input, output and feedforward vectors for each system at time k; A, B, C, D, E, F are the corresponding system matrices.

For the CFPP system, the input vector u includes the coal mass flow rate and the turbine governor valve, the output vector y includes the power output and the main steam pressure. The steam flow rate to the re-boiler is selected as the feedforward vector f.

For the PCC system, the input vector u includes the lean solvent flow rate and the steam flow rate to the re-boiler, the output vector y includes the CO_2 capture level and the re-boiler temperature. The flue gas flow rate of CFPP is selected as the feedforward vector f.

The prediction model (1) is identified through input-output data of the CFPP and PCC systems. In order to obtain identification data that can fully reflect the dynamics of the system, input signals as shown in Figs. 8 and 10 are designed to stimulate the CFPP and PCC systems respectively. Considering that the CFPP system responds faster than the PCC system, input signals are devised to change more frequently for the CFPP system. The generated output signals are shown in Figs. 9 and 11, in which the first half of data is used for identification and the remaining data is used for model validation. The sampling times of CFPP and PCC prediction models are selected as 10s and 30s, and the approach of subspace identification [38] is utilized to determine the prediction model, owing to its advantages in multi-variable, state-space model identification. The identification results are shown in Figs. 9 and 11.

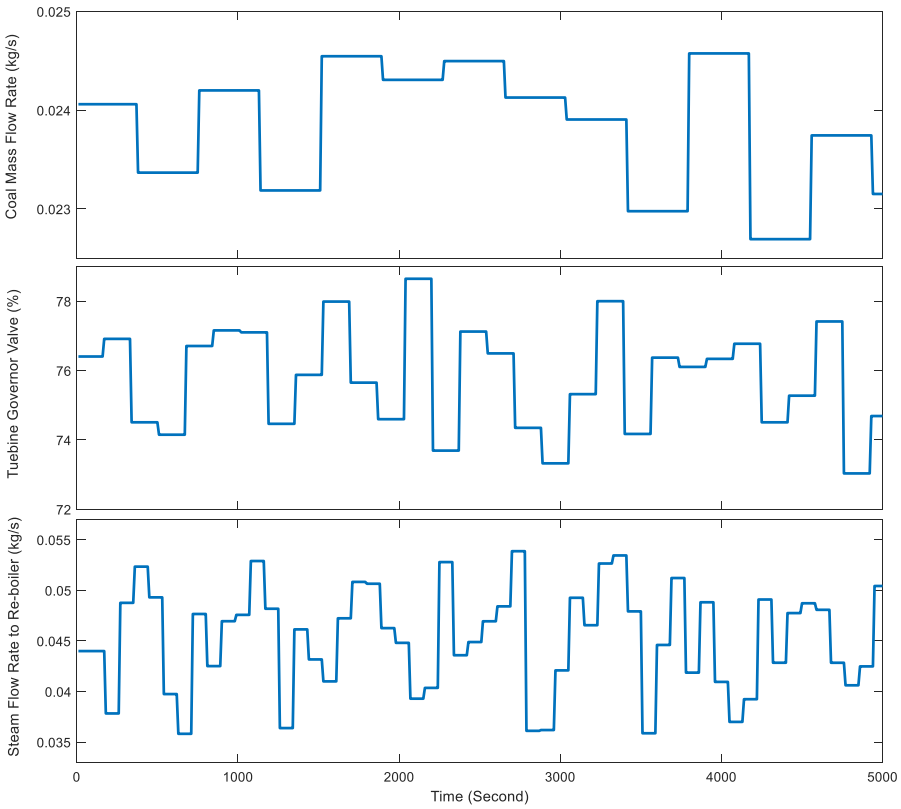

Fig. 8. Input signals used in CFPP prediction model identification.

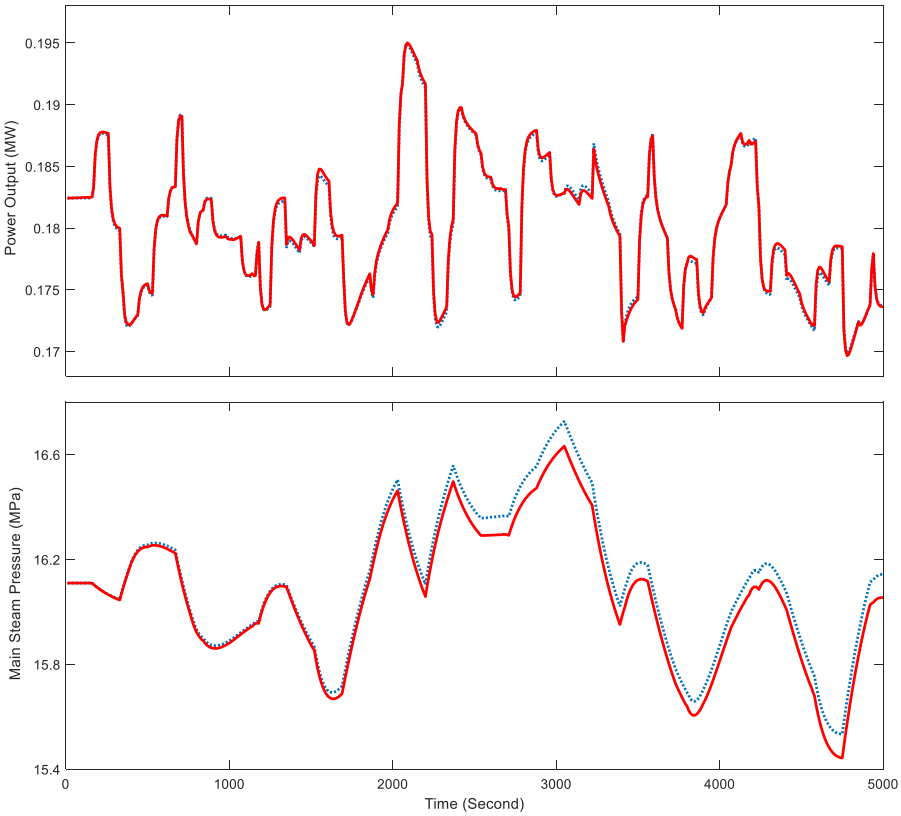

Fig. 9. Prediction model identification results for the CFPP system (solid in red: prediction model output; dotted in blue: simulator output).

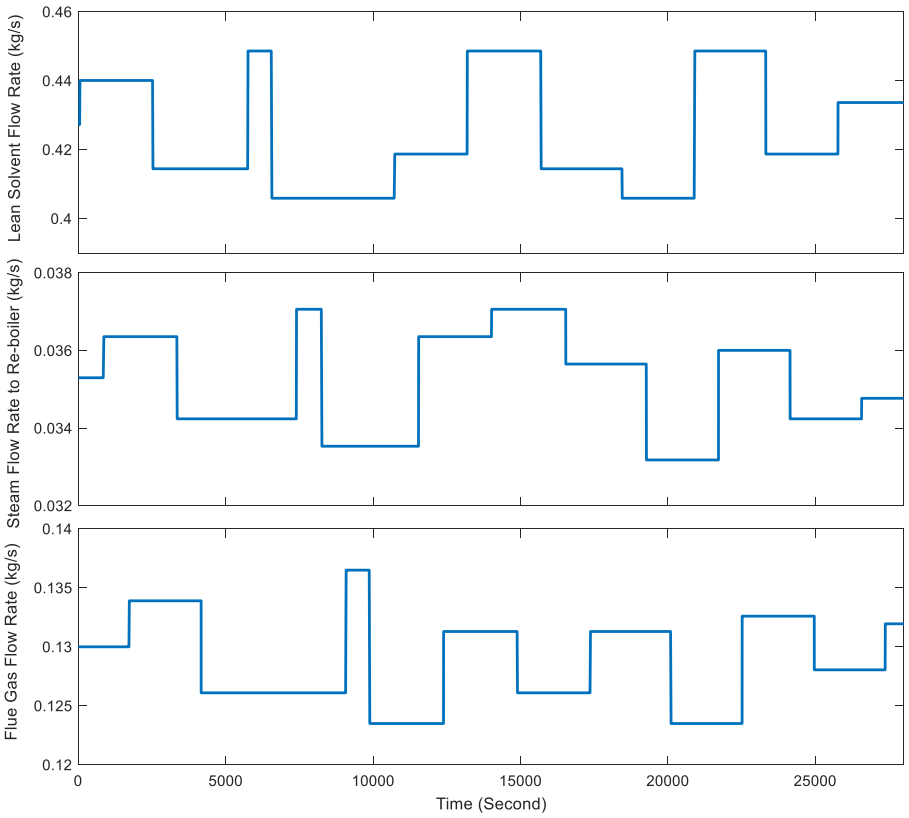

Fig. 10. Input signals used in PCC prediction model identification.

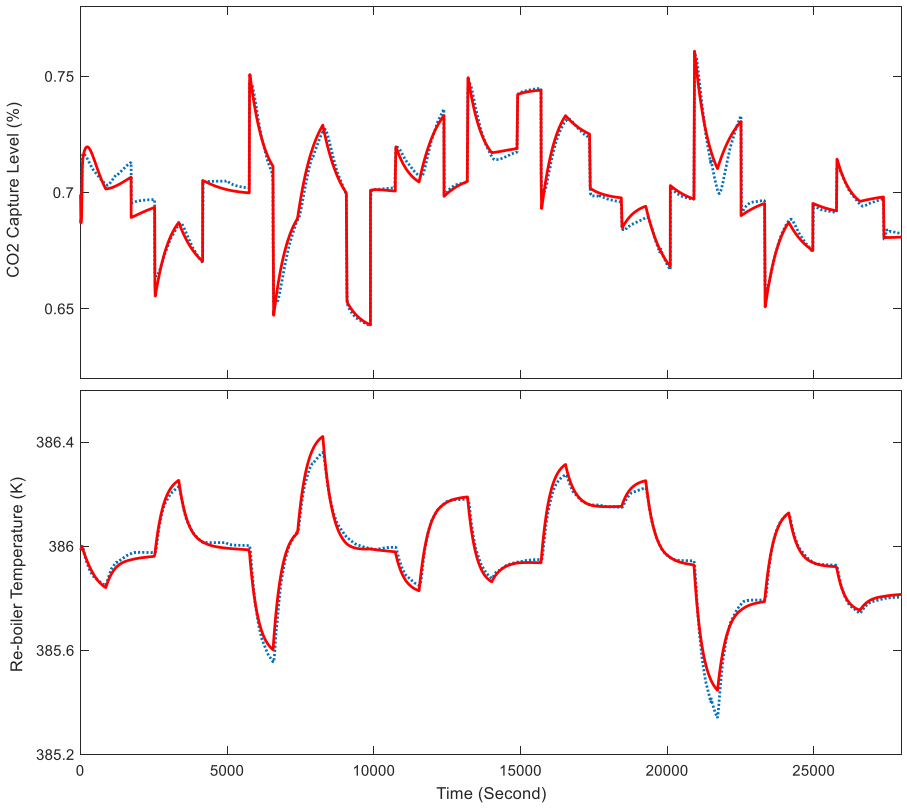

Fig. 11. Prediction model identification results for the PCC system (solid in red: prediction model output; dotted in blue: simulator output).

The results demonstrate that the identified models can reflect the dynamic behavior of the CFPP and PCC systems satisfactorily, thus they are selected as the prediction model in the coordinated MPCs design.

The prediction model (1) is then extended to an incremental style (2) to include integral action into the MPC, so that an

offset-free tracking effect can be attained in case of modeling mismatches:

$$\begin{cases} \begin{bmatrix} \Delta x_{k+1} \\ y_k \end{bmatrix} = \begin{bmatrix} A & 0 \\ C & I_2 \end{bmatrix} \begin{bmatrix} \Delta x_k \\ y_{k-1} \end{bmatrix} + \begin{bmatrix} B \\ D \end{bmatrix} \Delta u_k + \begin{bmatrix} E \\ F \end{bmatrix} \Delta f_k \\ y_k = \begin{bmatrix} C & I_2 \end{bmatrix} \begin{bmatrix} \Delta x_k \\ y_{k-1} \end{bmatrix} + D\Delta u_k + F\Delta f_k \end{cases} \tag{2}$$

in which Δx_k, Δu_k and Δf_k are the incremental values of the state, input, output and feedforward vectors, respectively, at time k, $\Delta x_k = x_k - x_{k-1}$, $\Delta u_k = u_k - u_{k-1}$, $\Delta f_k = f_k - f_{k-1}$.

By stacking up the predictive model (2) for N_y steps, the estimation of future output sequence $\hat{y}_f = \begin{bmatrix} \hat{y}_k^T & \hat{y}_{k+1}^T & \cdots & \hat{y}_{k+N_y-1}^T \end{bmatrix}^T$ within the prediction horizon N_y can be expressed by the future incremental input sequence $\Delta u_f = \begin{bmatrix} \Delta u_k^T & \Delta u_{k+1}^T & \cdots & \Delta u_{k+N_u-1}^T \end{bmatrix}^T$ and the prediction of future incremental feedforward signals $\Delta f_f = \begin{bmatrix} \Delta f_k^T & \Delta f_{k+1}^T & \cdots & \Delta f_{k+N_u-1}^T \end{bmatrix}^T$, where N_u is the control horizon, and is set to be shorter than N_y. We assume that the future control actions beyond control horizon N_u remains constant, i.e., $\Delta u_{k+N_u}^T, \ldots, \Delta u_{k+N_y-1}^T = 0$.

B. State estimation

Because the predictive model (1) is developed through data identification, the state vector x in the model does not have physical meanings and cannot be measured. For this reason, a state observer is designed to estimate its value based on the measured input, output and feedforward signals:

$$\begin{cases} \hat{x}_{k+1} = A\hat{x}_k + Bu_k + Ef_k + K(\hat{y}_k - y_k) \\ \hat{y}_k = C\hat{x}_k + Du_k + Ff_k \end{cases} \tag{3}$$

where the symbol "^" indicates the estimation, the observer gain K can be determined through the Lyapunov function method [39].

C. Optimization of the objective function

From the perspective of dynamic regulation, the objective of controller design is to track the given set-point rapidly and reduce the control action fluctuations as much as possible to ensure the smooth operation of the system. Thus the following quadratic objective function is considered in the MPC design:

$$J = (\hat{y}_f - r_f)^T Q_f (\hat{y}_f - r_f) + \Delta u_f^T R_f \Delta u_f \tag{4}$$

where $r_f = \begin{bmatrix} r_k^T & r_{k+1}^T & \cdots & r_{k+N_y-1}^T \end{bmatrix}^T$ is the desired set-points for the controlled variables; $Q_f = I_{N_f} \otimes Q_0, R_f = I_{N_u} \otimes R_0$ are the weighting matrices for the future CVs and MVs respectively.

At each sample, the objective function is minimized considering the constraints of input magnitude (5) and rate (6), and the optimal future incremental control sequence Δu_f can be calculated. The future control sequence u_f can then be obtained, and the first element u_k in the control sequence u_f is implemented on the CFPP-PCC system.

$$\begin{bmatrix} I_2 \\ I_2 \\ \vdots \\ I_2 \end{bmatrix} (u_{min} - u_{k-1}) \le \begin{bmatrix} I_2 & 0 & \cdots & 0 \\ I_2 & I_2 & \cdots & 0 \\ \vdots & \vdots & \ddots & \vdots \\ I_2 & I_2 & \cdots & I_2 \end{bmatrix} \Delta u_f \le \begin{bmatrix} I_2 \\ I_2 \\ \vdots \\ I_2 \end{bmatrix} (u_{max} - u_{k-1}) \tag{5}$$

$$\begin{bmatrix} I_2 \\ I_2 \\ \vdots \\ I_2 \end{bmatrix} \Delta u_{min} \le \Delta u_f \le \begin{bmatrix} I_2 \\ I_2 \\ \vdots \\ I_2 \end{bmatrix} \Delta u_{max} \tag{6}$$

Remark 4.1: The predicted future re-boiler steam flow rate sequence can be directly calculated by the MPC_PCC at each sample, which will be sent to the MPC_CFPP and used as the feedforward signal. Since the sampling period of MPC_PCC is three times longer than that of the MPC_CFPP, linear interpolation method is used to determine the estimated re-boiler steam flow rate sequence at intervals of 10s. Similarly, the predicted future coal mass flow rate sequence can be calculated by the MPC_CFPP at each sample, through which, the future flue gas flow rate can be estimated using an additional coal mass flow flue-gas model and sent to the MPC_PCC as feedforward signal. Because the prediction horizon of CFPP is shorter than that of PCC, we assume the future flue-gas flow rate beyond the prediction horizon of CFPP constant.

4.2 Three operation modes for controller design of the CFPP-PCC unit

The CFPP-PCC unit has a dual task of power generation and carbon reduction. In order to make full use of the integrated system in these two aspects, three operation modes are considered for the coordinated control system.

A. Normal operation mode

Under the normal operation mode, the set-points of the power generation and CO_2 capture level are provided by the scheduling layer and the coordinated control system is responsible for implementing rapid and smooth tracking of these set-points.

The set-points can be given by the experienced operators based on their personal preferences or given through economical optimizations based on a steady-state model of the CFPP-PCC unit, in which the coal price, electricity price, carbon price, government subsidies, etc., could be considered.

B. Rapid load change mode

In current electric power industry, various kinds of energy sources are used together. Among them, the conventional CFPPs have to undertake power grid's peak regulation task to alleviate the fluctuations caused by the intermittent renewable energy sources and varying load demand. This demand requires the CFPPs to change its power generation as fast as possible in a wide range imposing tighter requirements on the control of the CFPPs.

The dynamic behavior in Fig. 7 shows that by changing the steam flow rate to the re-boiler, the integrated CFPP-PCC system can quickly increase the power generation at the cost of reducing its carbon capture performance. Therefore, adjusting the steam flow rate to re-boiler becomes an additional means for power load regulation of CFPP unit. When running in the rapid load change mode, the CFPP controller receives the power generation instructions from the scheduling layer and the PCC controller is forced to change the re-boiler steam flow rate at the maximum rate until the power output of CFPP is close to its desired value. Under this mode, the MPC_PCC does not adjust the re-boiler steam flow rate to control the capture level, and the terms corresponding to these two variables are set to zero in the weighting matrices Q_0 and R_0. The PCC controller is only responsible for maintaining the re-boiler temperature closely around the given set-point to ensure the safe and optimal operation of PCC system.

C. Strict carbon capture mode

Following the current strict requirements on desulfurization and denitrification of the CFPP unit, it may be required for the CFPP to tightly control the CO_2 capture level around/beyond a certain limit in the future in order to meet the goal of carbon emission reduction.

For the PCC unit, the biggest disturbance is the change in the flue gas flow rate during the load-varying period of the CFPP. As shown in Figs. 4 and 5, the change of coal mass flow rate will cause the variation of flue gas flow rate, which will then change the capture level very quickly. One way to compensate for this disturbance is the timely adjustment of the lean solvent flow rate since it can also adjust the capture level quickly. However, the allowed change in the lean solvent flow rate is small for the safe operation of the PCC plant. Therefore, enforcing the rate constraints of coal mass flow rate and making the flue gas flow rate change match the rate limit of the lean solvent flow rate is the only way to avoid a drastic changes of CO_2 capture level during the load change of CFPP.

Under the strict CO_2 removal mode, the coordinated control system receives the power generation and CO_2 capture level set-points from the scheduling layer. For the MPC_CFPP, the rate constraints for coal mass flow rate will be enforced to avoid

the dramatic change of flue gas flow rate and its adverse effect on the PCC system operation. Because the MPC_CFPP's prediction of coal mass flow rate is used to estimate the future flue gas flow rate, the MPC_PCC system can perform actions in advance to better maintain the capture level and the re-boiler temperature.

5. Simulation Results

The effectiveness of the proposed CFPP-PCC coordinated control system is validated in this section through three case studies. The following parameters are set for the MPCs:

MPC_CFPP: sampling time T_s=10s, predictive horizon N_y=20, control horizon N_u=20. Considering that tracking the load demand is the primary task of the CFPP unit and the fluctuations of coal mass flow rate will have great impact on the PCC operation, the weighting matrices are set as Q_0=diag(15000, 1); R_0=diag(3000, 1). Input magnitude and rate constraints are given as: $u_{min}=\begin{bmatrix}0.01 & 50\end{bmatrix}^T$, $u_{max}=\begin{bmatrix}0.029 & 90\end{bmatrix}^T$; $\Delta u_{min}=\begin{bmatrix}-0.001/3 & -5/3\end{bmatrix}^T$, $\Delta u_{max}=\begin{bmatrix}0.001/3 & 5/3\end{bmatrix}^T$ due to the physical limitations of the valves.

MPC_PCC: sampling time T_s=30s, predictive horizon N_y=20, control horizon N_u=20. Since tracking the CO_2 capture level demand and maintaining the re-boiler temperature around optimal point are the main tasks of the PCC unit and the fluctuations of re-boiler steam flow rate will have great impact on the CFPP operation, the weighting matrices are set as Q_0=diag(50, 1); R_0=diag(5, 25). Input magnitude and rate constraints are given as: $u_{min}=\begin{bmatrix}0.2 & 0.005\end{bmatrix}^T$, $u_{max}=\begin{bmatrix}1 & 0.08\end{bmatrix}^T$; $\Delta u_{min}=\begin{bmatrix}-0.0035 & -0.0005\end{bmatrix}^T$, $\Delta u_{max}=\begin{bmatrix}0.0035 & -0.0005\end{bmatrix}^T$ due to the physical limitations of the actuators.

Case 1: The first case is presented to test the overall performance of the proposed coordinated MPCs under normal operation mode. We assume that at the beginning of the simulation, the CFPP_PCC system is operating at 0.2MWe power output, 15.88MPa main steam pressure, 80% CO_2 capture level and 386K re-boiler temperature condition. At t=300s and t=3300s, the power set-point changes to 0.225MWe and 0.13MWe respectively; and the CO_2 capture level set-point changes to 60% and 90% respectively, according to the instructions from the scheduling layer. The CFPP is operating at the sliding pressure mode, thus the main steam pressure set-point changes to 16.38 MPa and 13.60Mpa accordingly. The re-boiler temperature set-point is fixed at 386K, which is the optimal temperature for this PCC unit.

Two other controllers are used for comparison, which are:

A. Independent MPCs: Two MPCs with the same parameter settings are designed for the CFPP and PCC. However, the interactions between the two systems are not utilized; the steam flow rate to the re-boiler is not considered in the MPC_CFPP design and the flue gas flow rate is fixed at 0.13kg/s in the MPC_PCC design.

B. Conventional PI controllers: Boiler-following mode (using turbine governor valve to adjust the power output, coal mass flow rate to adjust the main steam pressure) is taken into account for the PI_CFPP design to achieve a rapid track of power demand. For the PCC system, the lean solvent flow rate is adopted to regulate the capture level, and the steam flow rate to re-boiler is adopted to regulate the re-boiler temperature. The parameters for the conventional PIs are set as follows:

Power control loop: P=30, I=0.8;

Main steam pressure control loop: P=0.0004, I=0.00004;

CO_2 capture level control loop: P= 0.006, I= 0.0015;

Re-boiler temperature control loop: P=0.07, I=0.0008.

The simulation results are shown in Figs. 12-15, they indicate the proposed coordinated MPCs can attain the best performance. When the power demand increases/decreases, the MPC_CFPP increases/decreases the coal mass flow rate and turbine governor valve on time, driving the power output of CFPP quickly to follow the desired value as shown in Figs. 12 and 13. The changing rate of the turbine governor valve is slower than that of coal mass flow rate, so that the dramatic reduction/increase of the main steam pressure can be avoided. On the other hand, as shown in Figs. 14 and 15, the MPC_PCC is well suited for adjusting the lean solvent and re-boiler steam flow rates to achieve a rapid reduction/increase of the capture level. The re-boiler temperature is kept closely around 386K to ensure an efficient operation of the PCC plant. Because the current flue gas flow rate and re-boiler

steam flow rate and their future predictions are used in the PCC and CFPP MPCs, the interactions between CFPP and PCC systems do not bring in a significant disturbance on the smooth operation of the entire plant.

The main difference of the independent MPCs from the proposed coordinated MPCs is that the interactions between CFPP and PCC systems is not taken into account for the independent MPCs. Owning to this reason, the tracking speed of power output, main steam pressure and CO_2 capture level are all slower for the independent MPCs as shown in Figs. 12 and 14. Moreover, these interactions bring severe disturbances into the CFPP and PCC control systems and greatly reduce the stability of both systems. It can be seen clearly in Figs. 13 and 15 that strong fluctuations occur for the independent MPCs.

Regarding the conventional PI controllers, sluggish responses of the overall system are observed in Figs. 12 and 14. Although the trend of the adjustments is reasonable, the single-loop based PI control cannot consider the interactions among multi-loops and provide the best control inputs. In addition, because of the past error-based control mechanism, it is difficult for the PI controllers to meet the prompt regulation requirement of the slow CFPP-PCC plant.

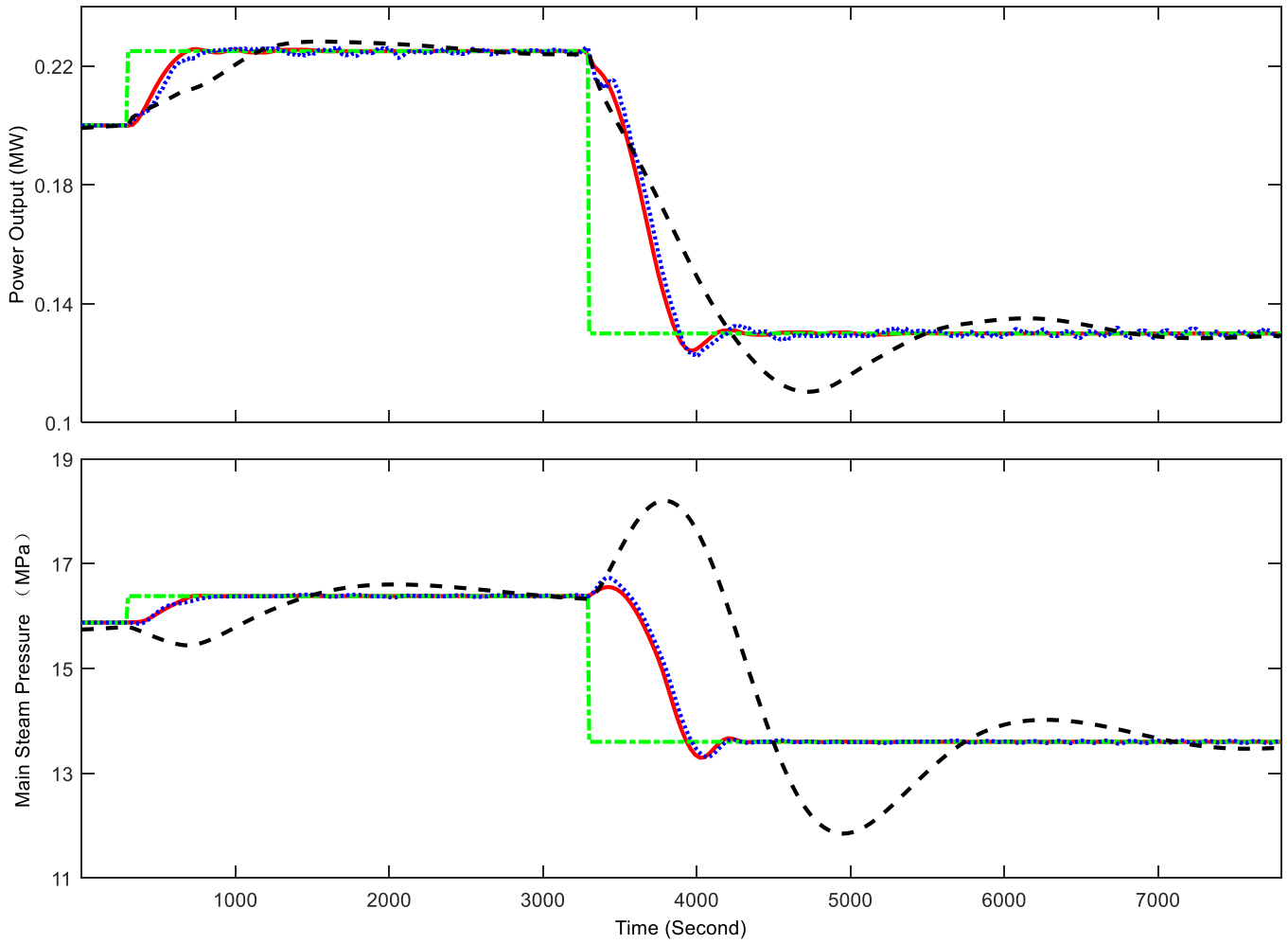

Fig. 12. Performance of the integrated CFPP-PCC system: CFPP output variables (solid in red: proposed coordinated MPCs; dotted in blue: independent MPCs; dashed in black: conventional PI controllers; dot-dashed in green: reference).

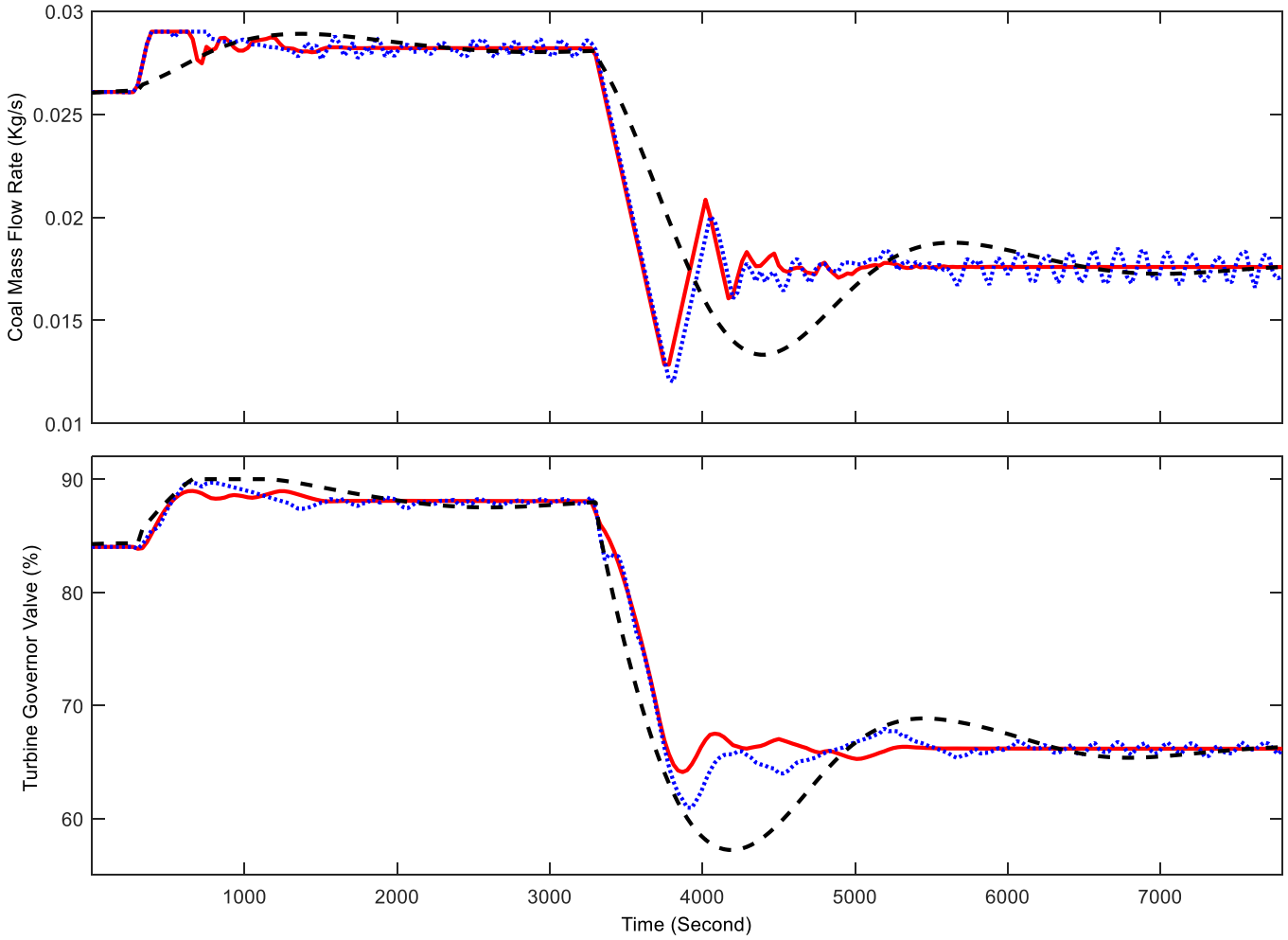

Fig. 13. Performance of the integrated CFPP-PCC system: CFPP manipulated variables (solid in red: proposed coordinated MPCs; dotted in blue: independent MPCs; dashed in black: conventional PI controllers).

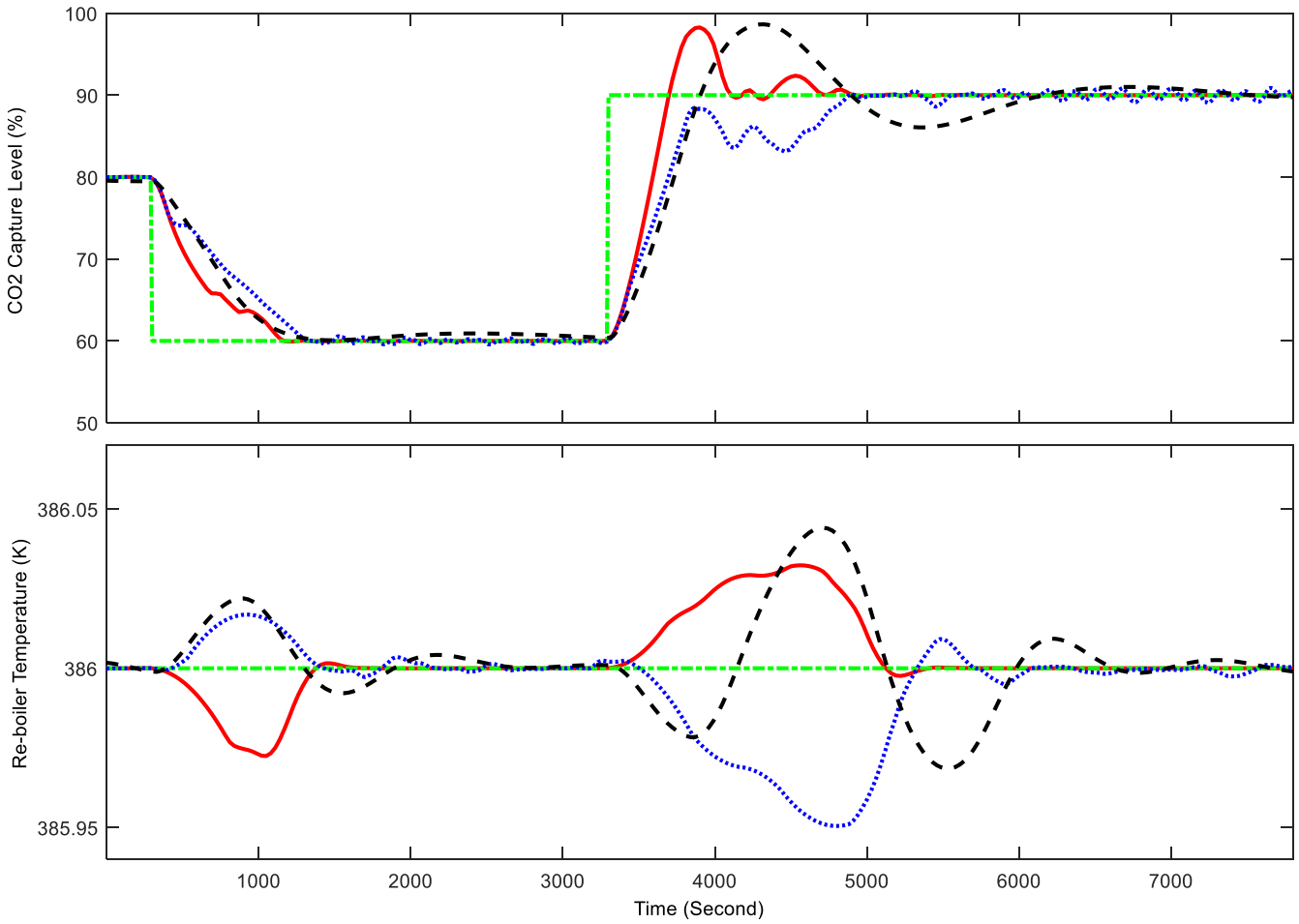

Fig. 14. Performance of the integrated CFPP-PCC system: PCC output variables (solid in red: proposed coordinated MPCs; dotted in blue: independent MPCs; dashed in black: conventional PI controllers; dot-dashed in green: reference).

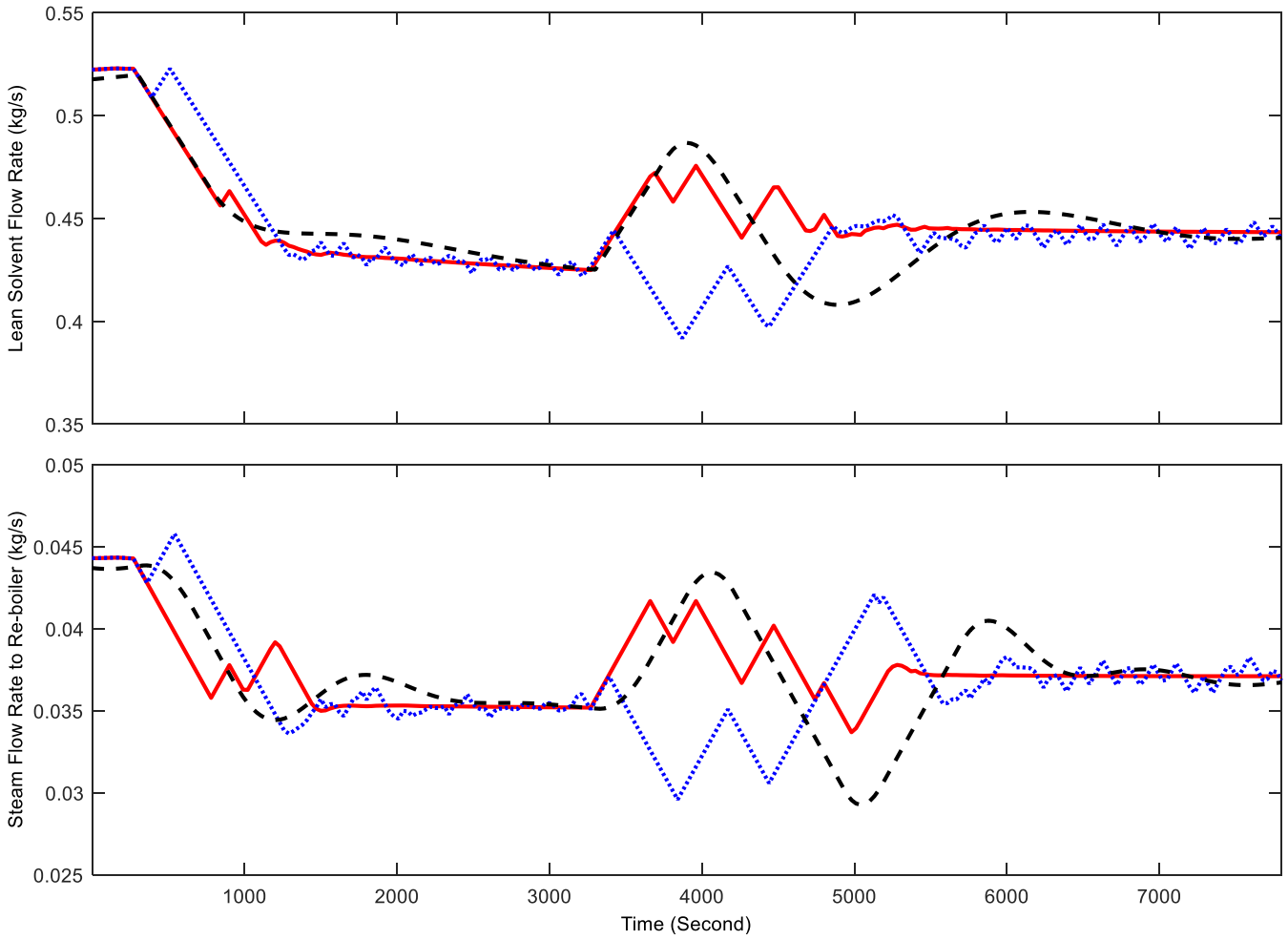

Fig. 15. Performance of the integrated CFPP-PCC system: PCC manipulated variables (solid in red: proposed coordinated MPCs; dotted in blue: independent MPCs; dashed in black: conventional PI controllers).

Case 2: The second simulation aims to present the performance of the proposed coordinated MPCs under the rapid power load change mode. We assume that at the beginning of the simulation, the CFPP-PCC system is operating at 0.17MWe power output, 14.70MPa main steam pressure, 70% CO_2 capture level and 386K re-boiler temperature condition. At t=300s, the power set-point increases to 0.21MWe, which is the most urgent need to track at the moment. The main steam pressure set-point also increases to 16.1 MPa, but the CO_2 capture level and re-boiler temperature set-points remain the same.

The proposed coordinated MPCs under normal operating mode, the independent MPCs under rapid power load change mode and the MPC of an individual CFPP unit are used for comparison to show the potential of CFPP-PCC unit in terms of power load regulation. The simulation results are shown in Figs. 16-19.

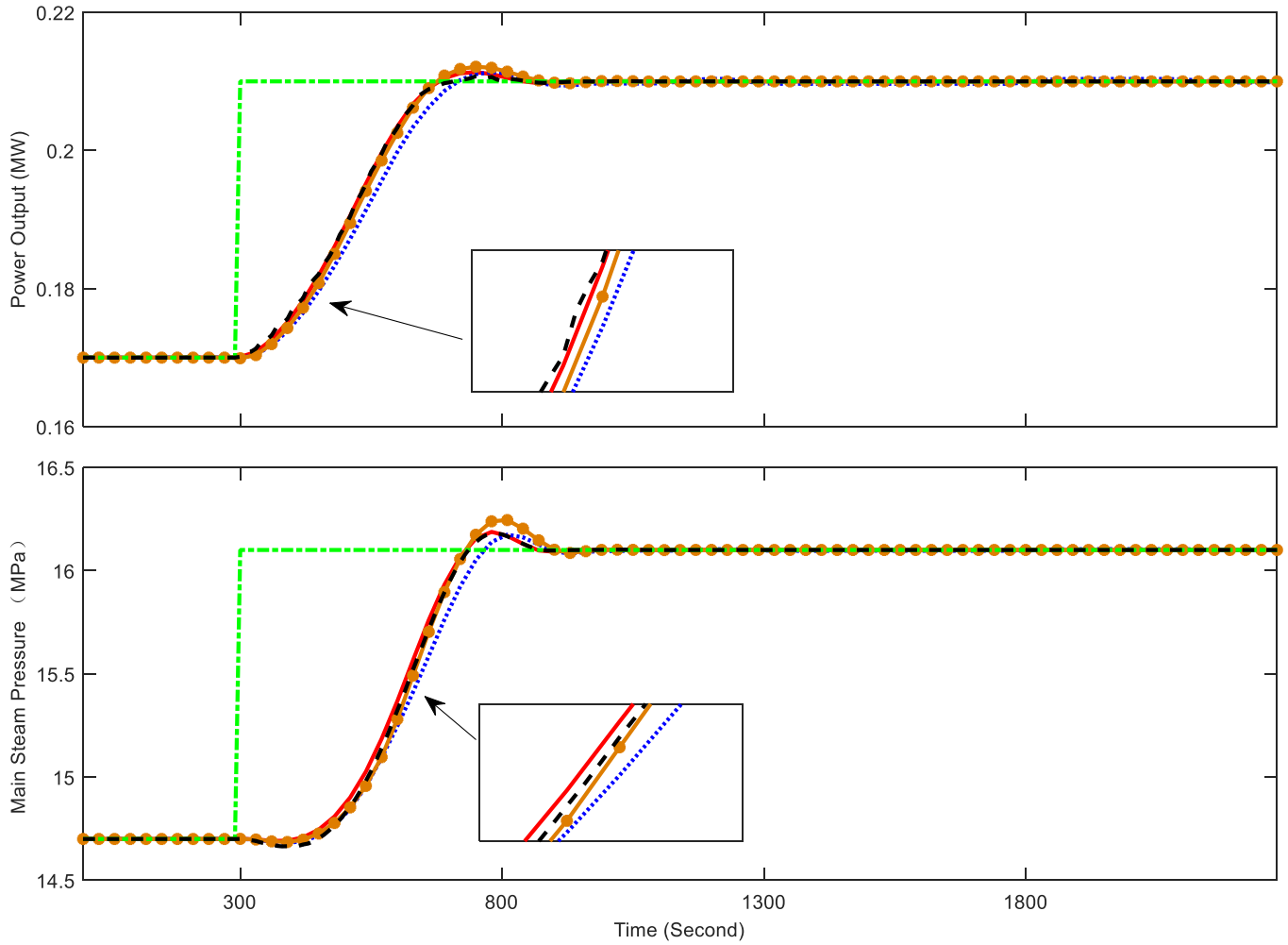

Fig. 16. Performance of the integrated CFPP-PCC system: CFPP output variables (solid in red: proposed coordinated MPCs under rapid power load change mode; dotted in blue: proposed coordinated MPCs under normal mode; dashed in black: independent MPCs under rapid power load change mode; circled in orange: conventional MPC of an individual CFPP unit; dot-dashed in green: reference).

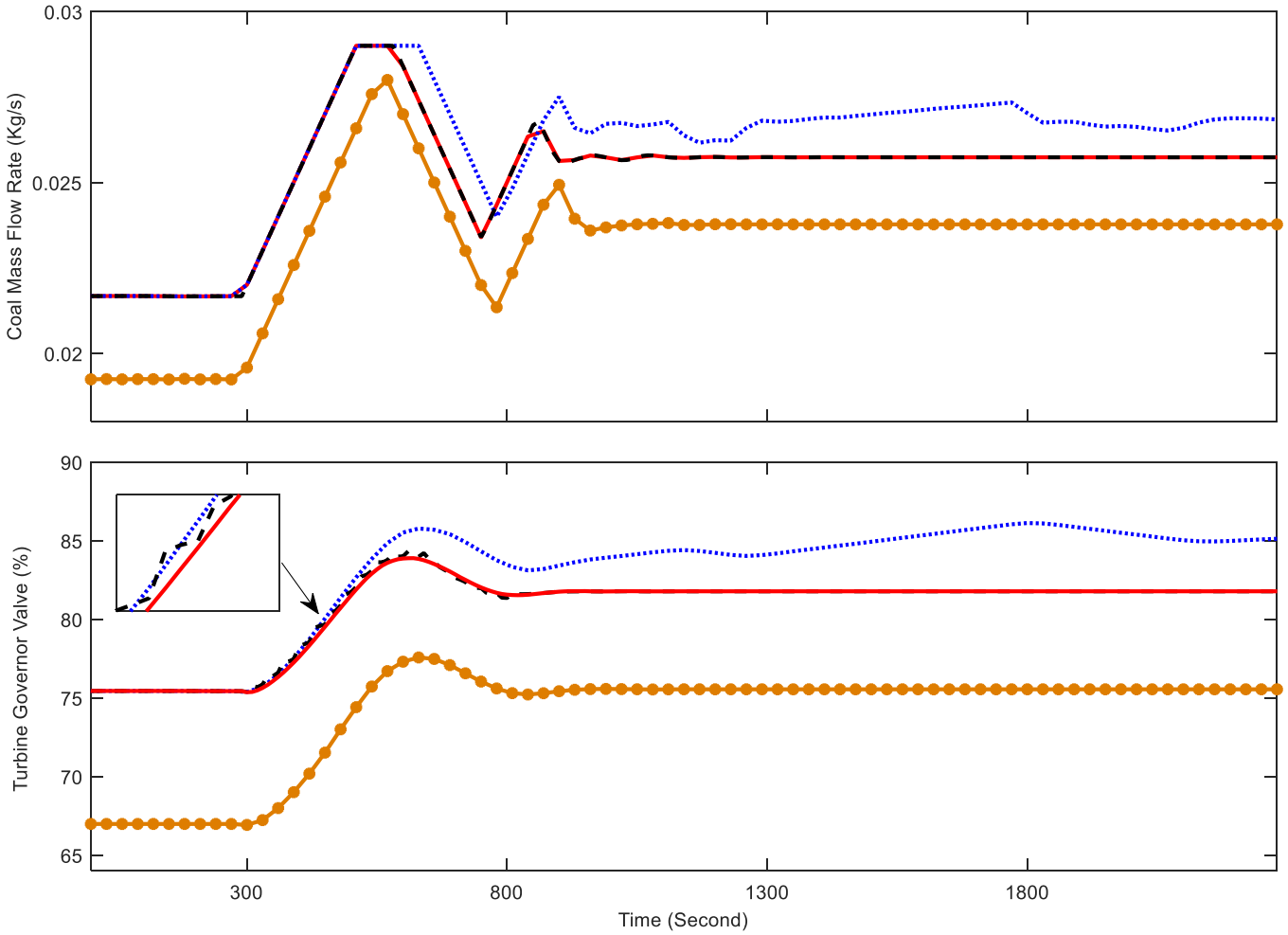

Fig. 17. Performance of the integrated CFPP-PCC system: CFPP manipulated variables (solid in red: proposed coordinated MPCs under rapid power load change mode; dotted in blue: proposed coordinated MPCs under normal mode; dashed in black: independent MPCs under rapid power load change mode; circled in orange: conventional MPC of an individual CFPP unit).

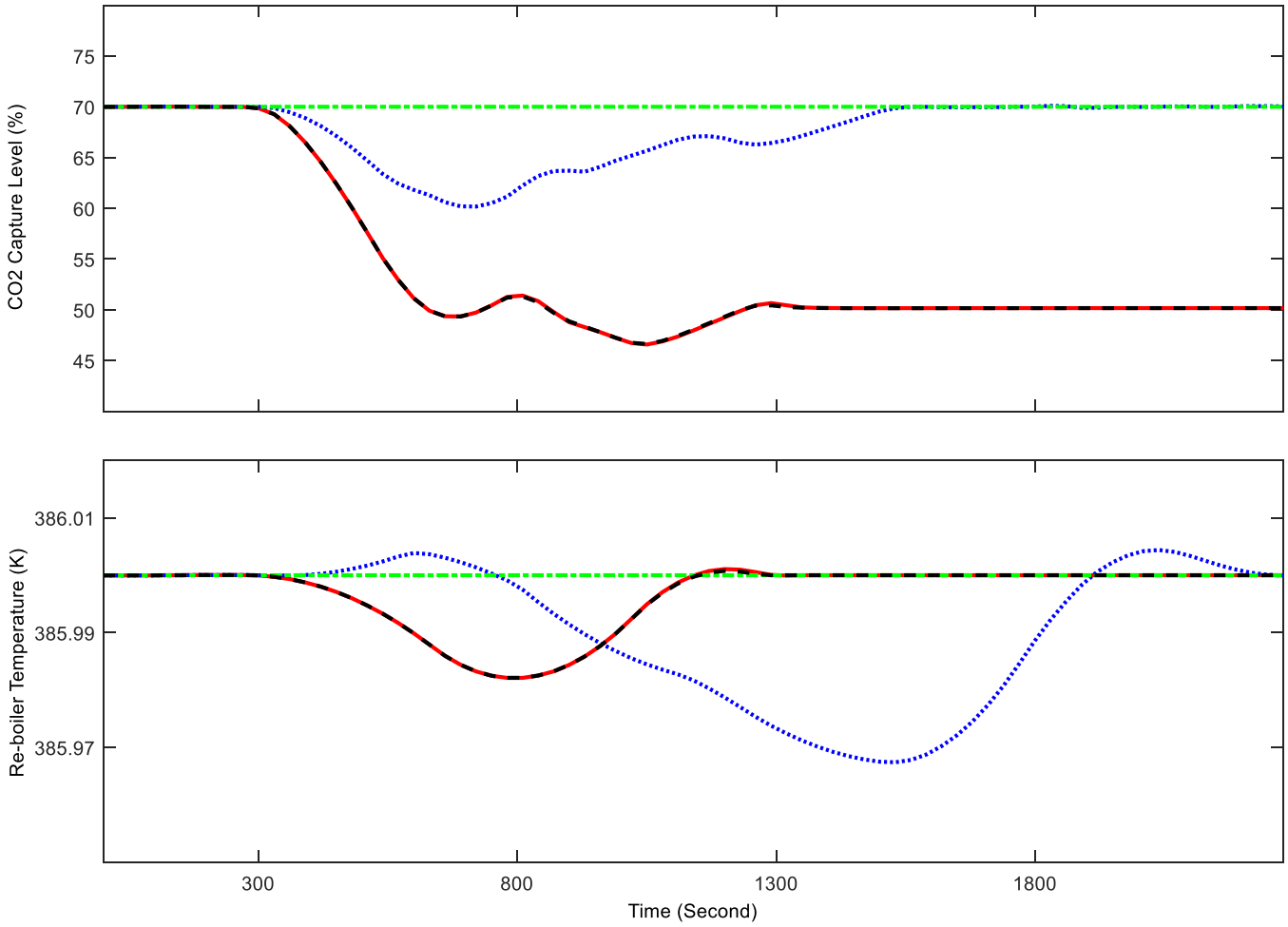

Fig. 18. Performance of the integrated CFPP-PCC system: PCC output variables (solid in red: proposed coordinated MPCs under rapid power load change mode; dotted in blue: proposed coordinated MPCs under normal mode; dashed in black: independent MPCs under rapid power load change mode; dot-dashed in green: reference).

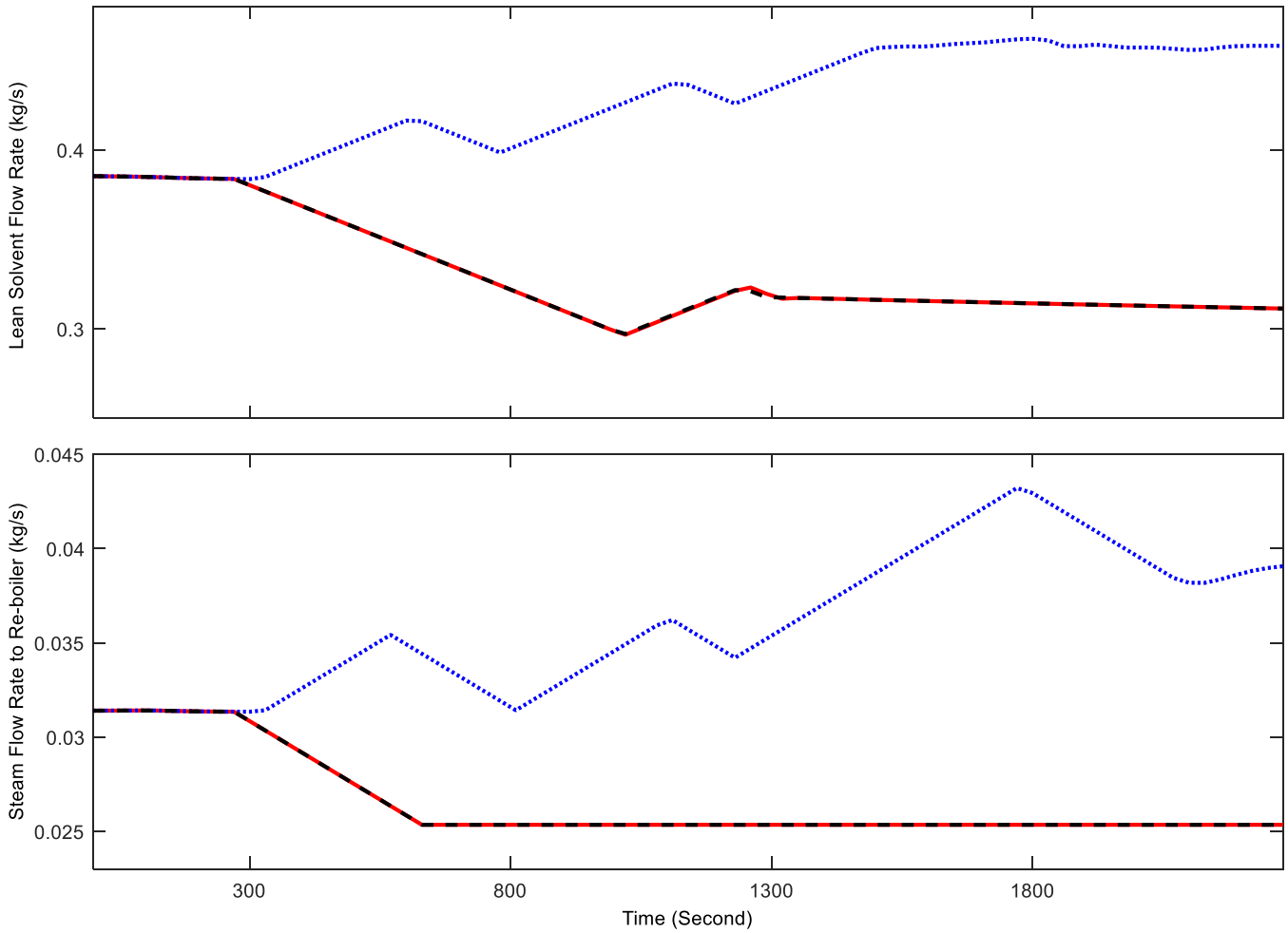

Fig. 19. Performance of the integrated CFPP-PCC system: PCC manipulated variables (solid in red: proposed coordinated MPCs under rapid power load change mode; dotted in blue: proposed coordinated MPCs under normal mode; dashed in black: independent MPCs under rapid power load change mode).

The simulation results show that a satisfactory power load increase can be achieved by proper rise of the coal mass flow rate and turbine governor valve for all three strategies. Among the four strategies, the proposed coordinated MPCs under the rapid power load change mode has the fast power load tracking response (shown in Fig. 16), because the steam drawn-off from the IP/LP turbine crossover has been reduced and used again for power generation in the LP turbine (shown in Fig. 19). Since an excellent power load tracking is now easier to achieve, the focus of MPC_CFPP is slightly biased towards steam pressure regulation under the same parameters. Smooth and prompt steam pressure tracking performance can be observed clearly under this mode in Fig. 16. Meanwhile, since the steam flow rate to re-boiler is forced to be reduced, the CO_2 capture level is out of control as shown in Fig. 18. The lean solvent flow rate is reduced corresponding to the re-boiler steam and flue gas flow rate as shown in Fig. 19. A good re-boiler temperature control can still be attained for the safe and optimal operation of PCC unit as shown in Fig. 18.

For the proposed coordinated MPCs under normal operating mode, the power load ramping is about 50s slower than that of the rapid power load change mode as shown in Fig. 16. The increase in power requires the CFPP controller to increase the coal mass flow rate, which will then gradually increase the flue gas flow rate and make a sudden reduction in CO_2 capture level as shown in Fig. 18. To maintain the capture level, more steam will be drawn-off from the turbine and the ramping of power load will thus be retarded.

A rapid power load tracking response can also be discovered for the independent MPCs under power load ramping mode. However, since the actions of PCC are not considered by the CFPP in the control design stage, the continuous reduction of re-boiler steam flow rate brings large unknown disturbances into the CFPP control system during the load change. As a result, fluctuations in turbine governor valve and power output can be observed in Figs. 17 and 16, which are harmful for the smooth operation of the CFPP. Regarding the PCC side, the performance of independent MPCs is similar to the coordinated MPCs under

the power load ramping mode. This is mainly because the CO_2 capture level is not controlled under this operating mode and the impact of flue gas flow rate on the re-boiler temperature is quite limited (as shown in Fig. 5). Therefore, even if the flue gas variation is unknown, a satisfactory re-boiler temperature control is easily achieved by adjusting the lean solvent flow rate.

The use of re-boiler steam in power generation also makes the ramping speed of CFPP-PCC unit faster than that of the individual CFPP unit controlled by the same MPC. This is clearly reflected in the early stage of regulation shown in Fig. 16. In the latter stage, the load varying rate of CFPP-PCC plant is gradually caught up by the individual CFPP. This is because the coal mass flow rate of CFPP-PCC system has already reached the upper limitation. For the individual CFPP unit, without the function of carbon capture, the coal consumption is less for the same power generation as shown in Fig. 17. Therefore, the magnitude constraint does not limit the optimization of coal mass flow rate during the power load increase. However, large overshoots can be viewed for the individual CFPP control in both power output and main steam pressure responses as shown in Fig. 16.

Case 3: The last simulation is presented to investigate the performance of the proposed coordinated MPCs under strict carbon capture mode. We assume that at the beginning of the simulation, the CFPP-PCC system is operating at 0.16MWe power output, 14.02MPa main steam pressure, 70% CO_2 capture level and 386K re-boiler temperature condition. At t=300s, the power set-point is increased to 0.21MWe and the main steam pressure set-point is increased to 16.1MPa. Then at t=1300s, the desired CO_2 capture level rises to 90% and the re-boiler temperature set-point remains the same during the simulation. Maintaining the capture level closely around the set-point during the power load rising is highly expected.

For the proposed coordinated MPCs under strict carbon capture mode, the rate constraint for the coal mass flow rate is strengthened to $-0.001/9 \leq \Delta u\_coal \leq 0.001/9$, one third of its original value. The proposed coordinated MPCs under normal operating mode and another conventional coordinated MPCs using only the current flue gas flow rate as a feedforward signal are used for comparison to show the CO_2 capture performance during power load change in the CFPP-PCC unit. The simulation results are shown in Figs. 20-23.

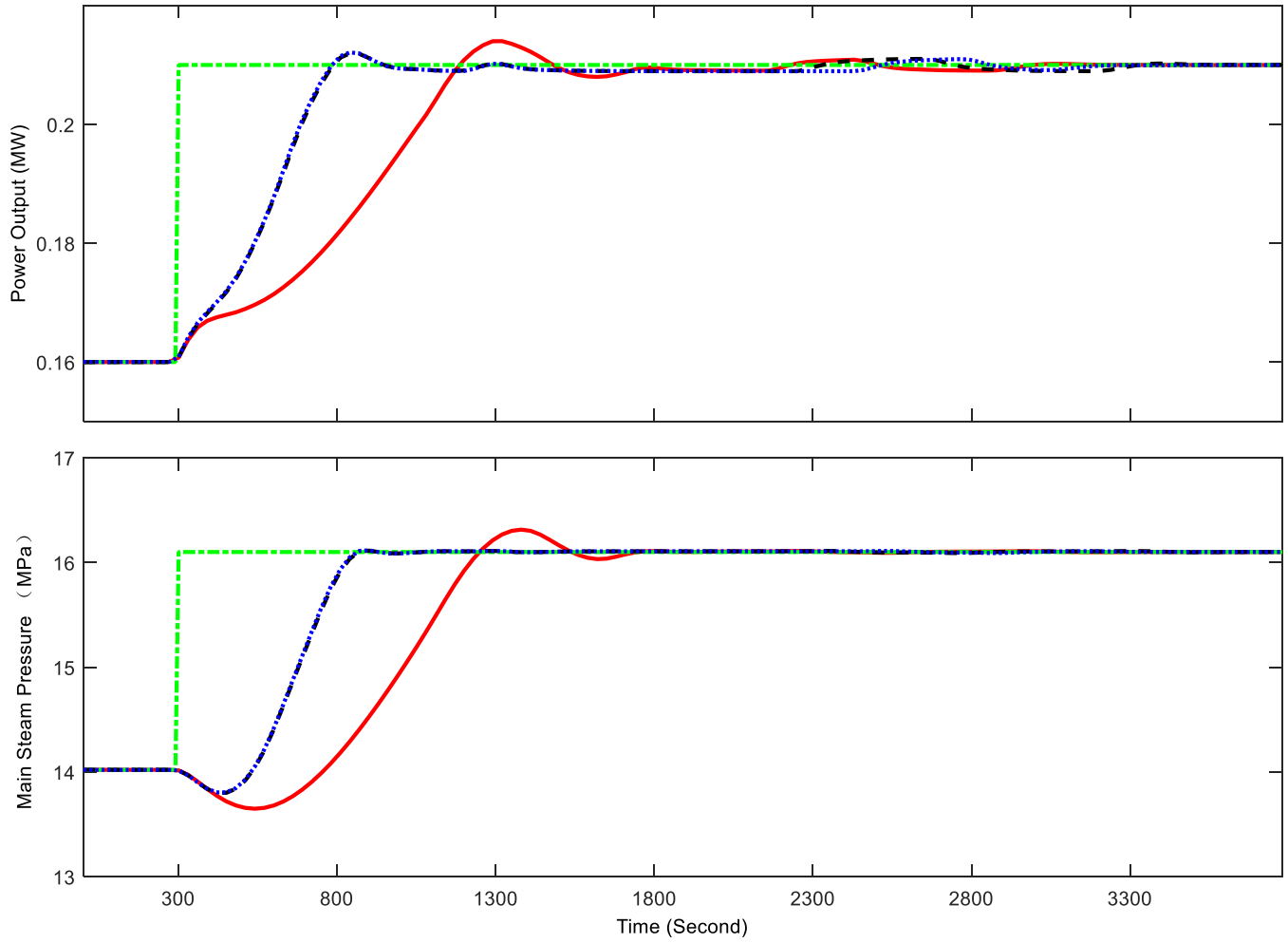

Fig. 20. Performance of the integrated CFPP-PCC system: CFPP output variables (solid in red: proposed coordinated MPCs under strict carbon mode; dotted in

blue: proposed coordinated MPCs under normal mode; dashed in black: conventional coordinated MPCs; dot-dashed in green: reference).

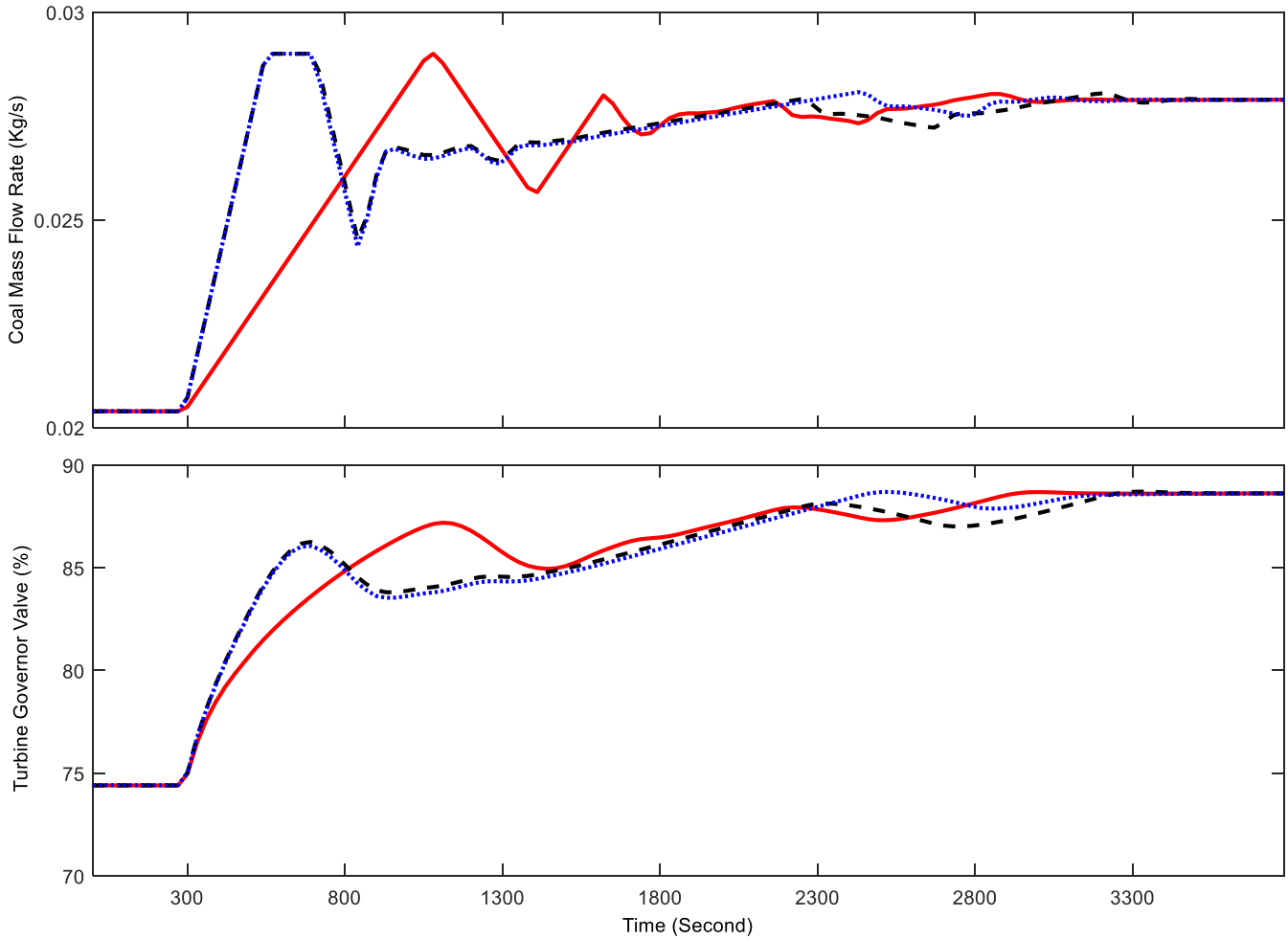

Fig. 21. Performance of the integrated CFPP-PCC system: CFPP manipulated variables (solid in red: proposed coordinated MPCs under strict carbon mode; dotted in blue: proposed coordinated MPCs under normal mode; dashed in black: conventional coordinated MPCs).

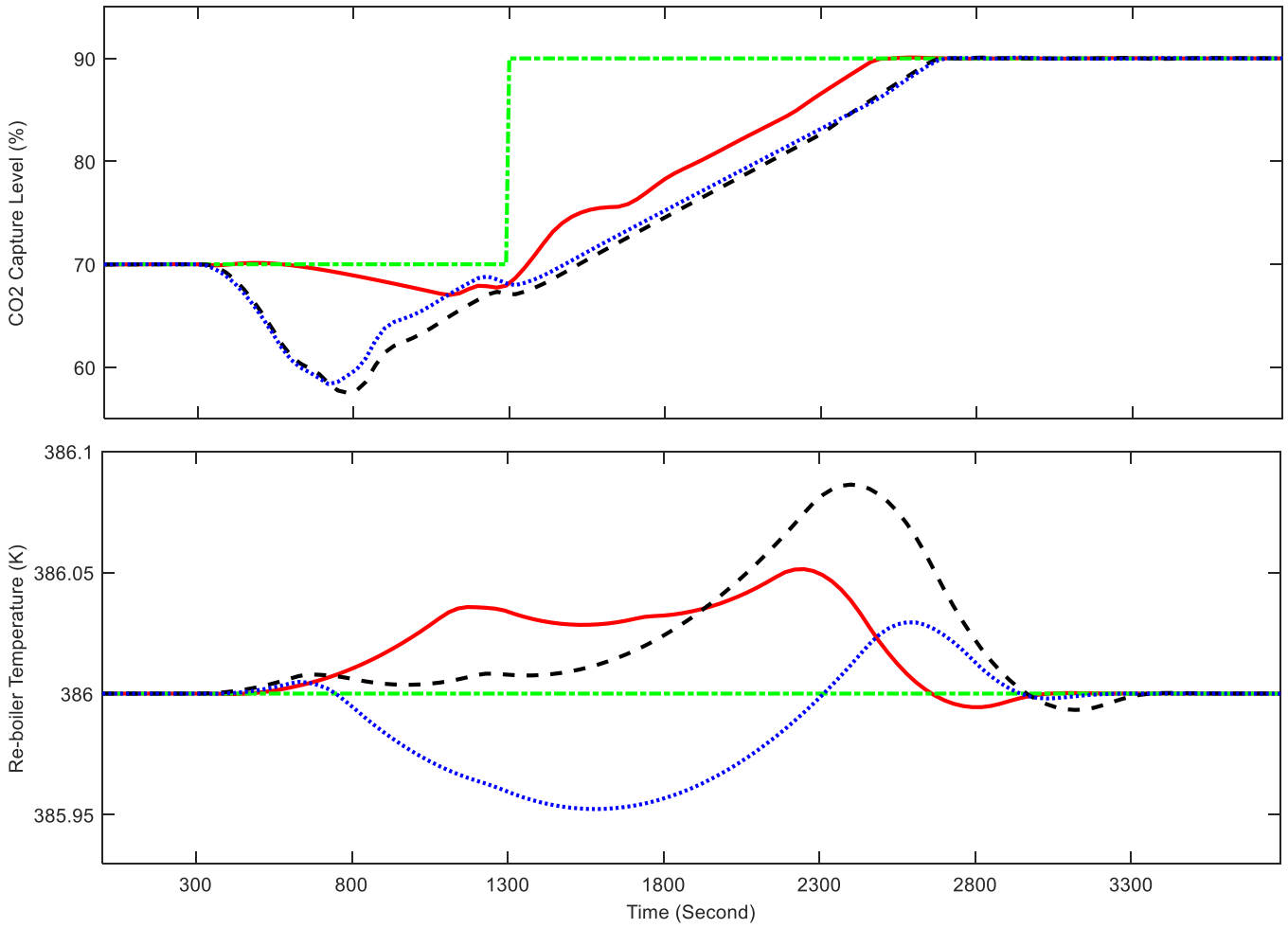

Fig. 22. Performance of the integrated CFPP-PCC system: PCC output variables (solid in red: proposed coordinated MPCs under strict carbon mode; dotted in blue: proposed coordinated MPCs under normal mode; dashed in black: conventional coordinated MPCs; dot-dashed in green: reference).

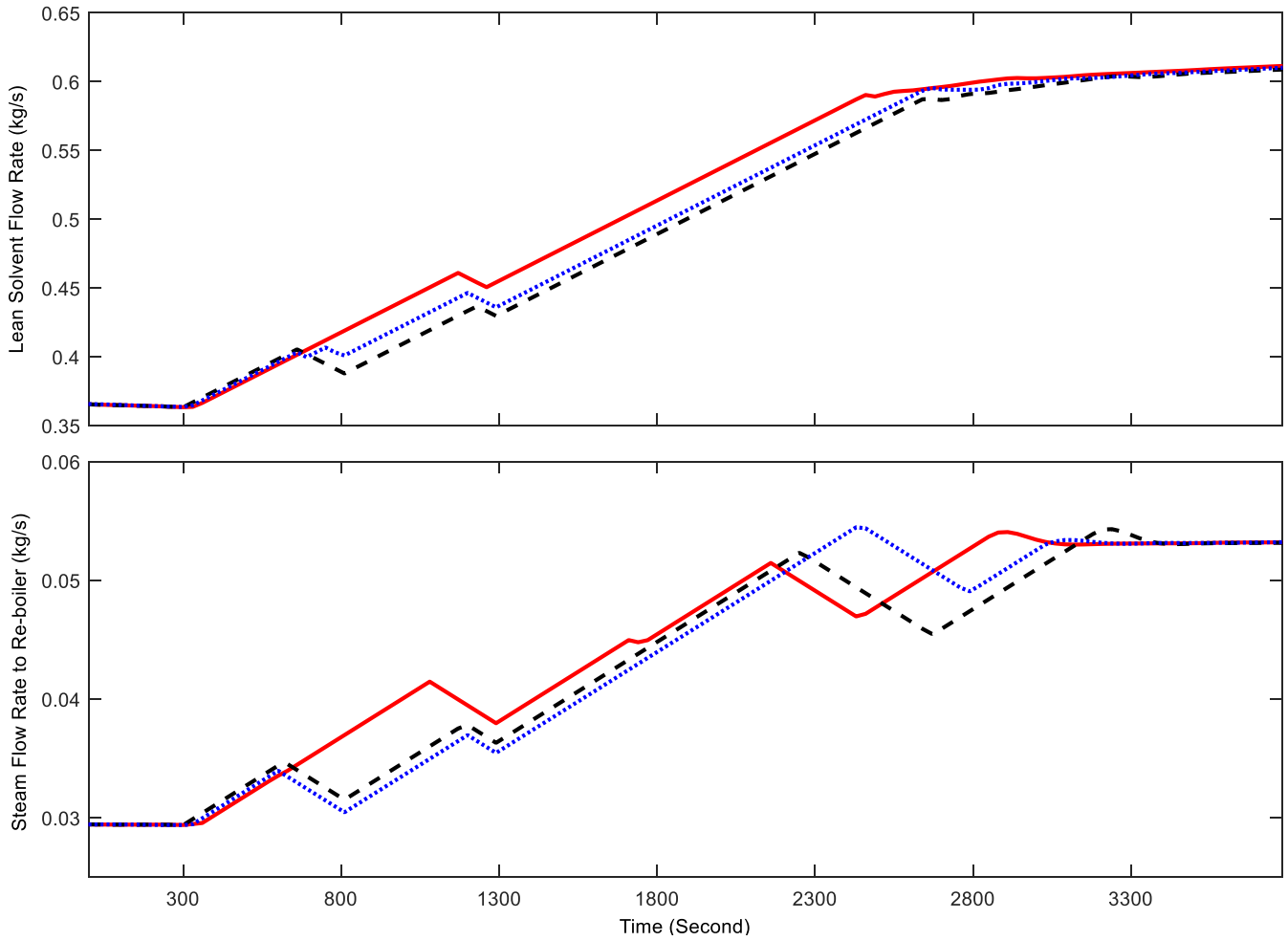

Fig. 23. Performance of the integrated CFPP-PCC system: PCC manipulated variables (solid in red: proposed coordinated MPCs under strict carbon mode; dotted in blue: proposed coordinated MPCs under normal mode; dashed in black: conventional coordinated MPCs).

In order to track the increased power commands, the CFPP control system has to increase the coal mass flow rate (shown in Fig. 21), which results in an increase of the flue gas flow rate. To avoid the decrease of CO_2 capture level as much as possible, the three control strategies all increase the lean solvent and re-boiler steam flow rate in general (shown in Fig. 23). Among the three strategies, the proposed coordinated MPCs under strict carbon capture mode has the smallest capture level control deviation (the biggest deviation is less than 3% before the capture level set point change) as shown in Fig. 22. This is achieved by strengthening the rate constraints of coal mass flow rate and slowing down the changing rate of flue gas flow rate as shown in Fig. 21. Although the power load tracking speed is reduced, the adjustments of PCC control system now can compensate the influence of flue gas in time. As comparison, for the proposed coordinated MPCs under nominal mode, much stronger capture level control deviation can be observed in Fig. 22 and the biggest deviation is more than 10% before the capture level set point change. Regarding the conventional coordinated MPCs, because only the current measured flue gas flow rate is sent to the PCC control, the future prediction feature of the MPC cannot be fully utilized. Worse capture level and re-boiler temperature control can be viewed clearly compared with the proposed coordinated MPCs as shown in Fig. 22.

The main purpose for selecting the strict carbon capture mode is to better maintain a given CO_2 capture level under the power plant load change. In case of capture level change, the coordinated MPCs under this mode cannot attain great advantages as shown in Fig. 22. The increase of capture level is mainly achieved by the increase of re-boiler steam and lean solvent flow rates. The response speed is thus subject to the behavior and constraints of the PCC system itself. Although the increase of re-boiler steam flow rate will make the CFPP increase the coal mass flow rate to maintain the given power output, the changing magnitude and rate are small. For this reason, strengthening the changing rate of coal mass flow rate cannot make much difference.

The three case studies show convincingly that the proposed coordinated MPCs in the three operating modes have significant

advantages in achieving the flexible operation of the integrated CFPP-PCC system and exerting its power generation and emission reduction capabilities.

6. Conclusion

There are strong interactions between the coal-fired power plant and the carbon capture system: the PCC re-boiler steam flow rate can change the CFPP power output rapidly and the CFPP coal mass flow rate will change the flue gas flow rate and bring in significant impact on the operation of PCC unit. Therefore, the control systems designed independently for each of the CFPP and PCC systems are not capable of handling the control issues of integrated system and maximize its functions in terms of power generation and carbon emission reduction.

To overcome this issue, this paper proposes a reinforced coordinated control structure for the integrated CFPP-PCC system. The foundation of the coordinated control is two sub-MPCs developed for each of the CFPP and PCC systems. The current flue gas and re-boiler steam flow rates and their future estimations are taken into account in the MPC design of PCC and CFPP, so that the interactions among the two sub-systems can be fully utilized by each MPC. Simulation results show that the proposed coordinated control strategy performs much better than the independent MPCs and conventional PI controls. Three operating modes are then proposed in the coordinated CFPP-PCC integrated control system design: the normal mode, the rapid power ramping mode and the strict carbon capture mode, to cover the full range of the entire system operation. It can be observed that under rapid power ramping mode, the CFPP can effectively improve its load-changing rate by using the re-boiler steam flow as an auxiliary regulation method; and under the strict carbon capture mode, by strengthening the rate limitations of coal mass flow rate, the given CO_2 capture level can be better maintained in the case of significant CFPP load change.

Acknowledgements

The authors would like to acknowledge the National Natural Science Foundation of China (NSFC) under Grant 51506029, the Natural Science Foundation of Jiangsu Province, China under Grant BK20150631, China Postdoctoral Science Foundation, EU FP7 International Staff Research Exchange Scheme on power plant and carbon capture (Ref: PIRSES-GA-2013-612230) and the Royal Society- Sino British Fellowship Trust International Fellowship for funding this work.

References

[1] EU, Global and European sea-level rise, from http://www.eea.europa.eu/data-and-maps/indicators/sea-level-rise-2/assessment, Accessed on 18th May 2018.

[2] UNFCCC, Historic Paris Agreement on Climate Change, from http://newsroom.unfccc.int/unfccc-newsroom/finale-cop21/, Accessed on 18th May 2018.

[3] IEA, The potential for carbon capture and storage in China, published on 17th Jan. 2017, from http://www.iea.org/newsroom/news/2017/january/the-potential-for-carbon-capture-and-storage-in-china.html, Accessed on 18th May 2018.

[4] M. Wang, A. Lawal, P. Stephenson, J. Sidders, and C. Ramshaw. Post-combustion CO_2 capture with chemical absorption: A state-of-the-art review. Chemical Engineering Research and Design, vol. 89, pp.1609-1624, 2011.

[5] E. S. Fernandez, M. Sanchez del Rio, H. Chalmers, P. Khakharia, E. L. V. Goetheer, J. Gibbins, and M. Lucquiaud. Operational flexibility options in power plants with integrated post-combustion capture. International Journal of Greenhouse Gas Control, vol. 48, pp. 275–289, 2016.

[6] M. T. Luu, N. A. Manaf, and A. Abbas, Dynamic modelling and control strategies for flexible operation of amine-based post-combustion CO2 capture systems, International Journal of Greenhouse Gas Control. vol. 39, pp. 377-389, 2015.

[7] A. Lawal, M. Wang, P. Stephenson, and O. Obi. Demonstrating full-scale post-combustion CO_2 capture for coal-fired power plants through dynamic modelling and simulation. Fuel, vol. 101, pp. 115-128, 2012.

[8] A. Aroonwilas and A. Veawab. Integration of CO2 capture unit using single- and blended-amines into supercritical coal-fired power plants: Implications for emission and energy management. International Journal of Greenhouse Gas Control, vol. 1, pp. 143-150, 2007.

[9] P. Galindo Cifre, K. Brechtel, S. Hoch, H. García, N. Asprion, H. Hasse, and G. Scheffknecht. Integration of a chemical process model in a power plant modelling tool for the simulation of an amine based CO2 scrubber. Fuel, vol. 88, pp. 2481-2488, 2009.

[10] T. Sanpasertparnich, R. Idem, I. Bolea, D. Montigny, and P. Tontiwachwuthikul. Integration of post-combustion capture and storage into a pulverized coal-fired power plant. International Journal of Greenhouse Gas Control, vol. 4, pp. 499-510, 2010.

[11] S. Oh, S. Yun and J. Kim. Process integration and design for maximizing energy efficiency of a coal-fired power plant integrated with amine-based CO2 capture process. Applied Energy, vol. 216, pp. 311-322, 2018.

[12] M. Lucquiaud, H. Chalmers, and J. Gibbins. Capture-ready supercritical coal-fired power plants and flexible post-combustion CO2 capture. Energy Procedia, vol. 1, pp.1411-1418, 2009.

[13] M. S. Rio, J. Gibbins and M. Lucquiaud. On the retrofitting and repowering of coal power plants withpost-combustion carbon capture: An advanced integration optionwith a gas turbine windbox. International Journal of Greenhouse Gas Control, vol. 58, pp. 299-311, 2017.

[14] D. Wang, S. Li, F. Liu, L. Gao, and J. Sui. Post combustion CO2 capture in power plant using low temperature steam upgraded by double absorption heat transformer. Applied Energy, vol. 227, pp. 603-612, 2018.

[15] M. Pan, F. Aziz, B. Li, S. Perry, N. Zhang, I. Bulatov and R. Smith. Application of optimal design methodologies in retrofitting natural gas combined cycle power plants with CO_2 capture. Applied Energy, vol. 161, pp. 695-706, 2016.

[16] T. Adams and N. Mac Dowell. Off-design point modelling of a 420 MW CCGT power plant integrated with an amine-based post-combustion CO_2 capture and compression process. Applied Energy, vol. 178, pp. 681-702, 2016.

[17] A. S. Brouwer, M. van den Broek, A. Seebregts and A. Faaij. Operational flexibility and economics of power plants in future low-carbon power systems. Applied Energy, vol. 156, pp. 107-128, 2015.

[18] J. Rodriguez, A. Andrade, A. Lawal, N. Samsatli, S. Calado, T. Lafitte, J. Fuentes, and C. Pantelides. An integrated framework for the dynamic modelling of solvent-based CO_2 capture processes, Energy Procedia vol.63, pp. 1206-1217, 2014.

[19] E. Mechleri, A. Lawal, A. Ramos, J. Davison, and N. M. Dowell. Process control strategies for flexible operation of post-combustion CO_2 capture plants, International Journal of Greenhouse Gas Control, vol. 57, pp. 14-25, 2017.

[20] N. Sipocz, F. A. Tobiesen and M. Assadi. The use of Artificial Neural Network models for CO_2 capture plants. Applied Energy, vol. 88, pp. 2368-2376, 2011.

[21] N. A. Manaf, A. Cousins, P. Feron, and A. Abbas. Dynamic modelling. Identification and preliminary control analysis of an amine-based post-combustion CO_2 capture pilot plant, Journal of Cleaner Production, vol. 113, pp. 635-653, 2016.

[22] R. Faber, M. Kopcke, O. Biede, J. N. Knudsen, and J. Andersen. Open-loop responses for the MEA post combustion capture process: Experimental results from the Esbjerg pilot plant, Energy Procedia, vol. 4, pp. 1427-1434, 2011.

[23] M. Bui, I. Gunawan, V. Verheyen, P. Feron, and E. Meuleman. Flexible operation of CSIRO's post-combustion CO_2 capture pilot plant at the AGL Loy Yang power station, International Journal of Greenhouse Gas Control, vol. 48, pp. 188-203, 2016.

[24] X. Wu, J. Shen, Y. Li, M. Wang, A. Lawal, and K. Y. Lee. Nonlinear dynamic analysis and control design of a solvent-based post-combustion CO2 capture process. Computers & Chemical Engineering, vol. 115, pp. 397-406, 2018.

[25] A. Lawal, M. Wang, P. Stephenson, G. Koumpouras, and H. Yeung. Dynamic modelling and analysis of post-combustion CO_2 chemical absorption process for coal-fired power plants, Fuel, vol. 89, pp. 2791-2801, 2010.

[26] Y. Lin, T. Pan, D. Wong, S. Jang, Y. Chi, and C. Yeh. Plantwide control of CO_2 capture by absorption and stripping using monoethanolamine solution. Ind Eng Chem Res, vol. 50, pp. 1338-1345, 2011.

[27] M. Panahi and S. Skogestad, Economically efficient operation of CO_2 capturing process part I: self-optimizing procedure for selecting the best controlled variables, Chemical Engineering and Processing: Process Intensification, vol. 50, no.3, pp. 247-253, 2011.

[28] T. Nittaya, P. L. Douglas, E. Croiset, and L. A. Ricardez-Sandoval. Dynamic modelling and control of MEA absorption processes for CO_2 capture from power plants. Fuel, vol. 116, pp. 672-691,2014.

[29] Q. Zhang, R. Turton, and D. Bhattacharyya. Development of Model and Model-Predictive Control of an MEA-Based Post combustion CO_2 Capture Process, Industrial & Engineering Chemistry Research, vol. 55, pp. 1292-1308, 2016.

[30] X. Wu, J. Shen, Y. Li, M. Wang, and A. Lawal, Flexible operation of post-combustion solvent-based carbon capture for coal-fired power plants using multi-model predictive control: a simulation study, Fuel, vol. 220, pp.931-941, 2018.

[31] A. Cormos, M. Vasile, and M. Cristea. Flexible operation of CO_2 capture processes integrated with power plant using advanced control techniques，12th International Symposium on Process Systems Engineering and 25th European Symposium on Computer Aided Process Engineering, Copenhagen, Denmark, May 31-Jun 4, 2015.

[32] A. K. Olaleye, E. Oko, M. Wang, and G. Kelsall. Dynamic modelling and analysis of supercritical coal-fired power plant integrated with post-combustion CO2 capture. Clean Coal Technology and Sustainable Development: Proceedings of the 8th International Symposium on Coal Combustion, pp. 359-363, Springer Science+ Business Media Singapore and Tsinghua University Press, Singapore, 2016.

[33] E. R. Dugas. Pilot plant study of carbon dioxide capture by aqueous monoethanolamine, M.S.E. Thesis, University of Texas at Austin; 2006.

[34] A. Lawal, M. Wang, P. Stephenson and H. Yeung. Dynamic modelling of CO_2 absorption for post combustion capture in coal-fired power plants, Fuel, vol. 88, pp. 2455-2462, 2009.

[35] J. Rodriguez, A. Andrade, A. Lawal, N. Samsatli, S. Calado, T. Lafitte, J. Fuentes and C. Pantelides. An integrated framework for the dynamic modelling of solvent-based CO_2 capture processes, Energy Procedia vol.63, pp. 1206-1217, 2014.

[36] J. Liu, S. Yan, D. Zeng, Y. Hu, and Y. Lv. A dynamic model used for controller design of a coal fired once-through boiler-turbine unit. Energy, vol. 93, pp. 2069–2078. 2015.

[37] X. Wu, J. Shen, Y. Li, and K. Y. Lee. Steam power plant configuration, design and control, WIREs Energy Environ, vol. 4, no. 6, pp. 537-563, Nov-Dec. 2015.

[38] S. Qin. An overview of subspace identification. Computers & Chemical Engineering, vol. 30, pp. 1502-1513, 2006.

[39] G. Feng. A survey on analysis and design of model-based fuzzy control systems. IEEE Transactions on Fuzzy Systems, vol. 14, no. 5, pp. 676-697, 2006.